Table 1
Quantitative analysis of the immunophenotype of BrdU+ cells

Marker	Control			Day 4			Day 9			Day 15		
	BrdU+ Cells[a]	Colabeled	Percentage[b]	BrdU+ Cells	Colabeled	Percentage	BrdU+ Cells	Colabeled	Percentage	BrdU+ Cells	Colabeled	Percentage
DG/SGZ												
Ki67	74	53	77	81	56	69	152	119	80	124	105	86
TUNEL	63	0	0	59	0	0	96	0	0	88	0	0
Musashi1	119	54	44	106	34	35	104	36	45	102	39	39
Nestin	83	12	14	62	12	17	88	18	20	79	16	20
βIII-Tubulin	102	0	0	94	0	0	185	4	2.2	176	5	2.8
TUC4	98	0	0	108	0	0	167	3	1.8	118	2	1.7
Doublecortin	107	0	0	106	0	0	183	4	2.2	154	4	2.4
Hu	95	0	0	100	0	0	107	1	1	104	1	1
NeuN	113	0	0	109	0	0	128	3	2.3	194	2	1
S100β	117	0	0	96	0	0	98	0	0	105	0	0
IT/SVZ												
Ki67	117	93	82	122	96	78	163	126	79	143	103	80
TUNEL	71	0	0	69	0	0	103	0	0	92	0	0
Musashi1	82	14	34	90	32	34	99	41	42	112	43	41
Nestin	74	12	17	91	12	13	73	11	15	89	17	19
βIII-Tubulin	94	0	0	96	0	0	134	4	3.1	153	4	2.8
TUC4	88	0	0	99	0	0	141	3	2.1	121	2	1.7
Doublecortin	101	0	0	102	0	0	139	3	2.1	161	3	1.8
Hu	84	0	0	92	0	0	118	2	1.8	123	3	2.4
NeuN	91	0	0	89	0	0	151	2	1.4	168	2	1.2
S100β	111	0	0	100	0	0	160	11	7	173	12	7

[a] Total BrdU+ cells scanned.
[b] BrdU+/Marker+ cells as a percentage of total BrdU+ cells scanned.

section) and also did not colocalize with BrdU (Figs. 2R and S; Table 1).

Immunophenotype of BrdU+ cells

Neural progenitor cells were labeled with antibodies against the RNA-binding protein Musashi1 and the intermediate filament protein Nestin. Musashi1 and Nestin are enriched in embryonic neural progenitor cells (Sakakibara et al., 1996; Kaneko et al., 2000; Lendahl et al., 1990) as well as in reactive astrocytes in the adult brain (Duggal et al., 1997; Yagita et al., 2001). We found BrdU/Musashi1 or BrdU/Nestin double-positive cells in SGZ and SVZ of all monkeys (Figs. 3A–H). The percentage of BrdU+ cells colabeled by these markers in SGZ and SVZ was 35–45% for Musashi1 and 15–20% for Nestin (Table 1) with no significant differences among the monkeys. Further, we observed Musashi1+/glial fibrillary acid protein (GFAP)+ and Nestin+/GFAP+ cells in SGZ and SVZ, but these were BrdU-negative (arrow in Figs. 3A,C, and F).

To investigate whether proliferating cells acquire the immunophenotype of neuronal progenitors, we performed fluorescent double immunostaining for BrdU and each of four proteins—βIII-tubulin (Lee et al., 1990), TUC(TOAD/Ulip/CRMP)4 (Quinn et al., 1999), doublecortin (Gleeson et al., 1999; Francis et al., 1999), and Hu (Okano and Darnell, 1997)—previously shown to be preferentially expressed in early postmitotic neurons. We observed double-labeled cells only in the postischemic Days 9 and 15 monkey DG and IT. In DG, the BrdU+ cells that were colabeled with TUC4 (Fig. 3I), βIII-tubulin (Fig. 3J), or doublecortin (Fig. 3K) displayed a similar location and appearance: they were located within SGZ and had an elongated shape and extended processes along the granule cell layer. In SVZ and adjacent white matter, the BrdU+ cells coexpressing doublecortin (Fig. 3L), βIII-tubulin (Fig. 3O), and TUC4 (Fig. 3P) had a similar fusiform shape and processes oriented radially to the lumen of the later ventricle. In contrast, the BrdU+/Hu+ cells were localized to the deep layers of the neocortical gray matter (Fig. 3M). The double-labeled cells accounted for approximately 1–3% of the BrdU+ cells in DG and IT of either the Day 9 or Day 15 monkeys (Table 1).

As we had seen for the neuronal progenitor markers, we observed BrdU+ cells that were double-stained for either NeuN or S100β, only in the Days 9 and 15 postischemic monkeys. In DG, the BrdU+/NeuN+ cells were localized to the granule layers adjacent to SGZ (Fig. 3R), while in the gray matter of IT to layers II–IV (Fig. 3S). They composed 1–2% of the BrdU+ cells scanned (Table 1). None of the NeuN+ cells in the ischemia-vulnerable CA1 sector coexpressed BrdU (Fig. 2Q). The BrdU+/S100β+ astrocytes in IT of the Days 9 and 15 monkeys (Fig. 3T) were severalfold more numerous than the BrdU+/NeuN+ cells (Table 1). In contrast, the astrocytes in DG, either GFAP+ (Figs. 3A,C, and F) or S100β+ (Table 1), did not colabel with BrdU.

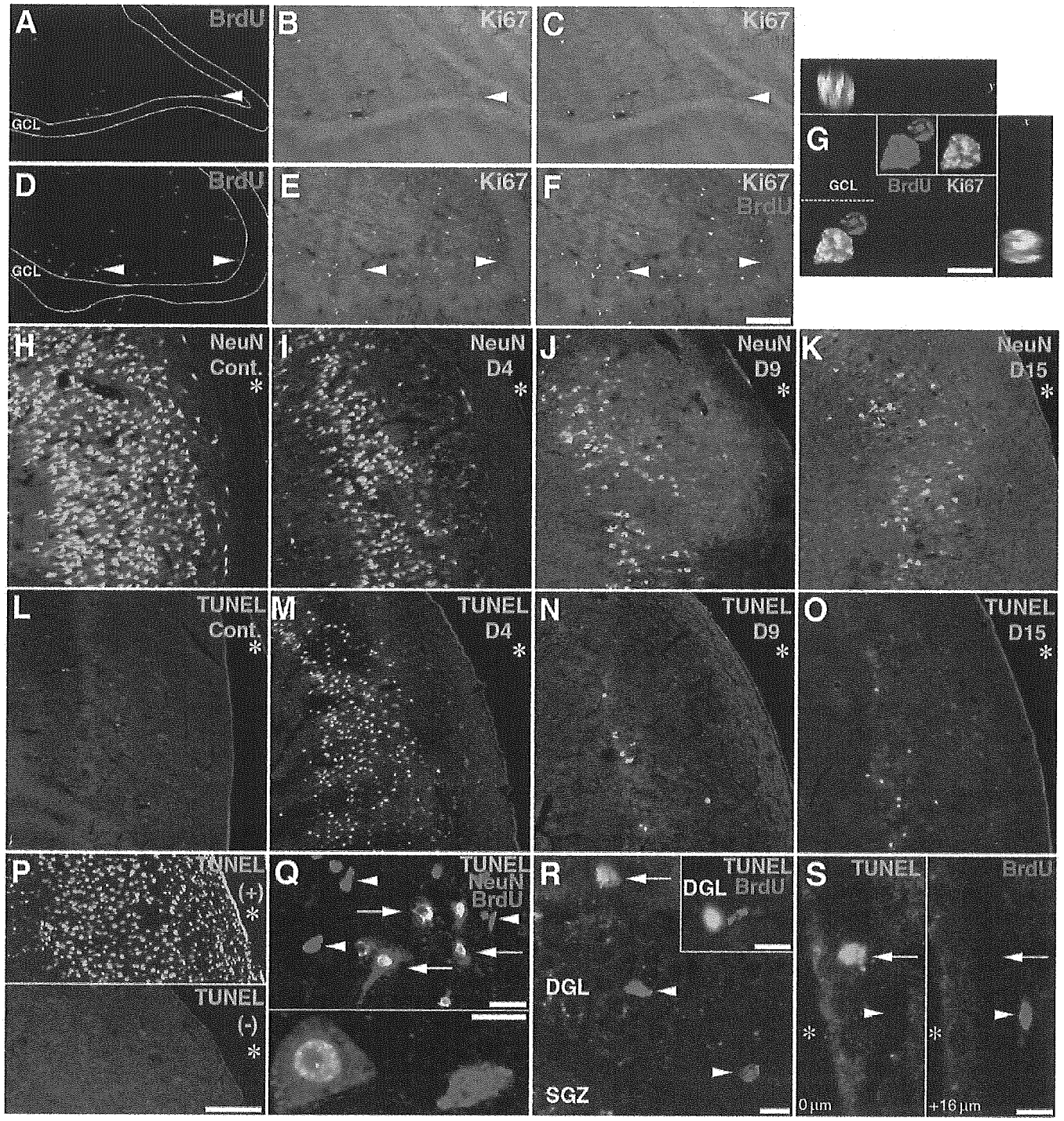

Fig. 2. BrdU/Ki67 double staining in control (A–C) and postischemic Day 9 (D–F) DG. While most BrdU+ nuclei are colabeled, a few BrdU+/Ki67- cells are present as well (arrowheads). Digital reconstructions confirm the colocalization of the BrdU and Ki67 signals in the same nucleus (G). NeuN immunohistochemistry in the hippocampal CA1 sector (H–K) visualizes the marked neuronal loss after ischemia. TUNEL staining in the same sector (L–O) shows that the bulk of DNA damage occurs in the first postischemic days, with only a few TUNEL+ cells at postischemic Days 9 and 15. Positive and negative controls confirm the specificity of the TUNEL reaction (P). TUNEL/NeuN/BrdU triple labeling (Q) in the CA1 sector (Day 4) demonstrates that the TUNEL+/NeuN+ CA1 neurons (arrows) and the BrdU+ cells (arrowheads) do not colocalize. (R and S) TUNEL and BrdU label different cells also in DG and SVZ (Day 9). Asterisk, inferior horn of the lateral ventricle; DGL, dentate granule layer. Scale bars: A–F (in F), H–P (in P), 200 µm; Q, 20 µm; G, R, and S (in S), 10 µm.

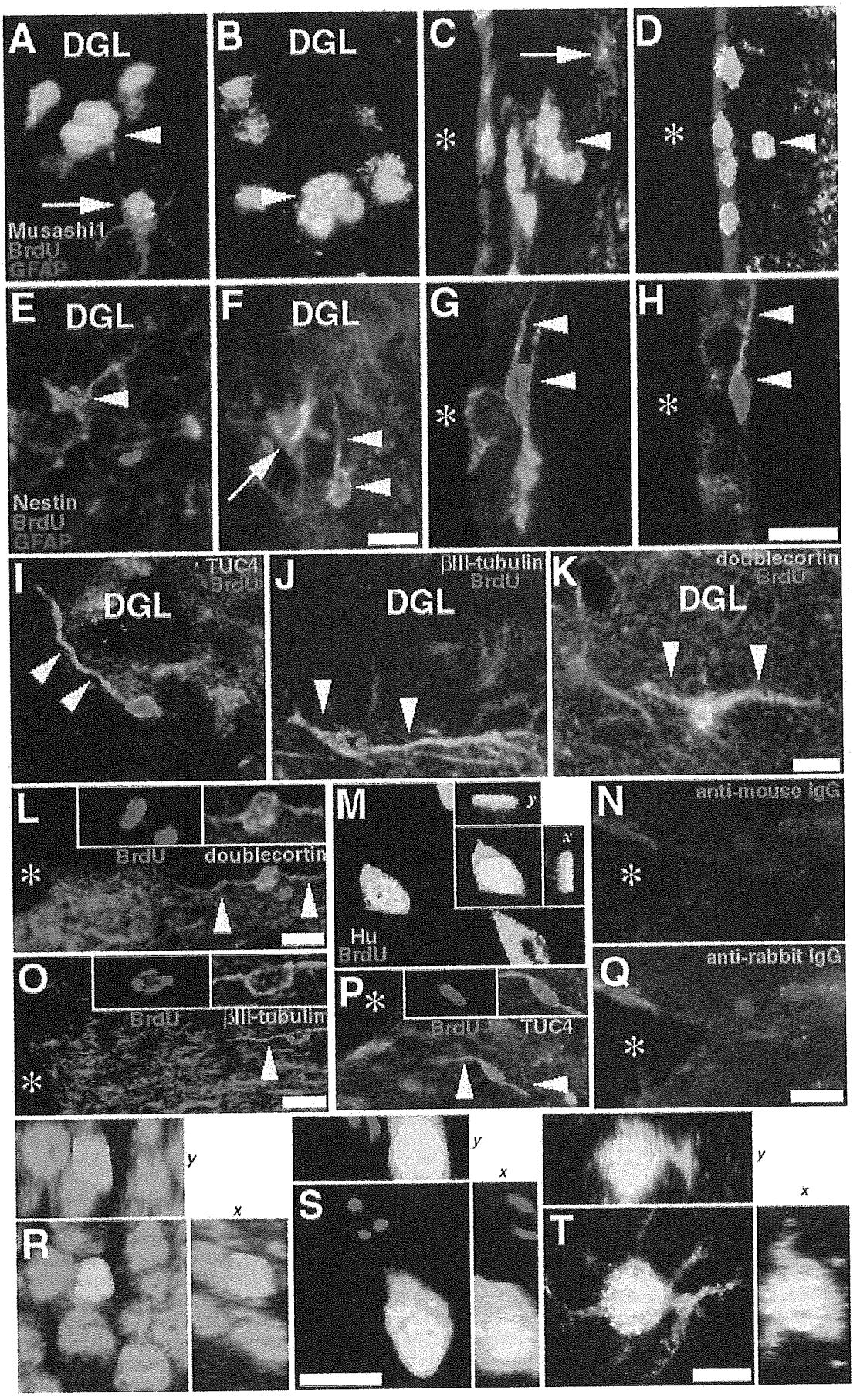
A DGL
Musashi1
BrdU
GFAP
B DGL
C
D
E DGL
Nestin
BrdU
GFAP
F DGL
G
H
I DGL
TUC4
BrdU
J DGL
βIII-tubulin
BrdU
K DGL
doublecortin
BrdU
L
BrdU
doublecortin
M
y
x
Hu
BrdU
N
anti-mouse IgG
O
BrdU
βIII-tubulin
P
BrdU
TUC4
Q
anti-rabbit IgG
R
y
x
S
y
x
T
y
x

Discussion

Our study provides the first evidence that brain ischemia in young adult primates increases the production of neural progenitors in SGZ and SVZ, and induces de novo generation of cells with neuronal and glial immunophenotype in DG and IT (Fig. 4). Cell proliferation increased in the second week after the ischemic insult (Days 9 and 15). These findings are compatible with the findings in rodents (Liu et al., 1998; Takagi et al., 1999; Yagita et al., 2001), in which proliferation in DG peaks 8–11 days after global ischemia. However, the density of BrdU+ cells in the postischemic monkey DG was about a tenth of that seen in the rodent (Liu et al., 1998; Yagita et al., 2001), despite the use of a much higher BrdU dose in the monkey.

BrdU selectively labels proliferating cells

As BrdU is an indicator of DNA synthesis, not a direct mitotic marker, its incorporation into newly synthesized DNA can occur not only during the S-phase of the cell cycle preceding cell division, but also during the repair of damaged DNA (Rakic, 2002). Particularly, brain ischemia/reperfusion leads to elevated DNA damage (Liu et al., 2001), and thus the possibility that BrdU is taken up by cells during the repair of this damage should be considered. Two lines of evidence in the current study suggest that BrdU selectively labels dividing cells. (1) Most BrdU+ cells were colabeled by an independent proliferation marker, Ki67. BrdU+ cells were more numerous than Ki67+ cells probably because the latter represent only the fraction of cells proliferating at the time of animal sacrifice, while BrdU was incorporated within a period of 96 h. (2) BrdU was not integrated by cells undergoing DNA damage as revealed by TUNEL assay. Previously, Cooper-Kuhn and Kuhn (2002) demonstrated that at a dose of 50 mg/kg, BrdU is not incorporated by TUNEL+ cells in the normal adult rodent SVZ. The lack of BrdU/TUNEL colabeling in our study at a BrdU dose of 500 mg/kg (total per monkey) suggests that a magnitude higher BrdU regimen still selectively labels proliferating cells under the current BrdU immunohistochemistry protocol. Further, the colocalization of BrdU with Ki67 (a protein endogenous to the cells) argues against the possibility that the elevated BrdU reaction after ischemia results from postischemic increase of the blood–brain barrier permeability. A recent study comparatively quantitated BrdU+ vs Ki67+ cells in the postischemic rodent DG and found that the latter are more numerous in the former 1 day after BrdU injection (Kee et al., 2002). In our study, the lifetime of BrdU+ cells was up to 4 days, thus allowing some of them (the BrdU+/Ki67− cells) to exit the active cell cycle. This might explain the larger number of BrdU+ cells than Ki67+ cells.

Upregulation of neural progenitor cell proliferation after ischemia

While Musashi1 and Nestin are enriched in embryonic neural progenitors, in adults they are abundantly expressed in astrocytes (Sakakibara et al., 1996; Kaneko et al., 2000; Lendahl et al., 1990; Duggal et al., 1997). Thus, in adults, it is important to distinguish Nestin+ or Musashi1+ astrocytes from precursor cells. Two recent reports (Yagita et al., 2001; Takasawa et al., 2002) demonstrated that clusters of BrdU+ cells in the postischemic rat SGZ coexpress Musashi1 but not GFAP, although a few BrdU+/GFAP+ cells outside the clusters could be found. Here we showed that neither the BrdU+/Musashi1+ nor the BrdU+/Nestin+ cells colocalized with GFAP, in either SGZ or SVZ. Seri et al. (2001) presented evidence that GFAP+ cells are the earliest BrdU-incorporating cells in the mouse SGZ and that these cells subsequently generate neurons. The differences between their results and ours may be due to the different survival times after BrdU incorporation and/or to species variations. We assume that in the adult primate, the populations of BrdU+/Musashi1+/GFAP− and/or BrdU+/Nestin+/GFAP− cells represent neural precursor cells. The percentage of BrdU+ cells that were colabeled with either Musashi1 or Nestin did not vary significantly among the experimental groups. However, as the total number of BrdU+ cells was significantly increased in the postischemic Days 9 and 15 SGZ/SVZ, they contained significantly more proliferating neural progenitors than the control SGZ/SVZ.

Postischemic proliferation of neuronal precursors

Cells that were double-positive for BrdU and TUC4, βIII-tubulin, doublecortin, or Hu, which are all proteins that are expressed by young postmitotic neurons, were found only in the two groups (Days 9 and 15) that showed increased mitotic activity as well. This finding suggests that cell proliferation and neuronal differentiation were concom-

Fig. 3. Immunophenotype of BrdU+ cells. (A–H) BrdU incorporation into neural progenitors. Musashi1+ cells incorporate BrdU (arrowheads) in both the control (A) and postischemic (B and D, Day 15; C, Day 4) DG (A and B) and SVZ (C and D). Nestin+ cells incorporate BrdU (arrowheads) in both the control (E and G) and postischemic (F and H, Day 9) DG (E and F) and SVZ (G and H). The Musashi1+/GFAP+ (A and C) and Nestin+/GFAP+ (F) cells are not colabeled by BrdU (arrows). (I–P) BrdU incorporation into neuronal precursor cells. BrdU+/TUC4+ (I, Day 15), BrdU+/βIII-tubulin+ (J, Day 9), and BrdU+/doublecortin+ (K, Day 9) cells extending processes (arrowheads) in SGZ. BrdU+/doublecortin+ (L, Day 9), BrdU+/βIII-tubulin+ (O, Day 9), and BrdU+/TUC4+ (P, Day 15) cells extending processes (arrowheads) in SVZ and adjacent white matter. (M) A Hu+/BrdU+ cell in the IT (gray matter, Day 9) with digital reconstructions of the cell in the x and y axes. Omission of primary antibodies eliminates immunoreactivity (N and Q). (R–T) BrdU/NeuN colabeling in Day 9 DG (R) and Day 15 IT (S) and BrdU/S100β colabeling in Day 9 IT (T) with three-dimensional reconstructions. DGL, dentate granule cell layer; asterisk, inferior horn of the lateral ventricle. Scale bars: A–F (in F), G–H (in H), I–K (in K), L, R–T, 10 μm; M–Q, 20 μm.

itantly upregulated by ischemia. The proliferating cells expressing TUC4, βIII-tubulin, or doublecortin in SGZ or SVZ were similar in their appearance and relative abundance, suggesting that they represented the same cell type. However, the fraction of proliferating neuronal precursors in the postischemic monkey SGZ was much lower than in that of the postischemic rodent at comparable survival times after BrdU treatment (Kee et al., 2001; Takasawa et al., 2002). In IT, BrdU+/Hu+ cells were restricted to the gray matter, in contrast to the BrdU+/TUC4+, BrdU+/doublecortin+, and BrdU+/βIII-tubulin+ cells. This may indicate differential expression patterns by neuronal progenitors at different stages of their maturation.

As TUC4 and doublecortin were reported to be expressed also in nonneuronal cells (Nacher et al., 2000; Mizuguchi et al., 1999), we carefully analyzed the BrdU+ cells coexpressing either of the two proteins—only double-positive cells with bipolar morphology characteristic for immature neurons were included in the statistics. Further, a nonneuronal expression of Hu and βIII-tubulin has not been reported to our knowledge, compatible with our observations. Thus, it is unlikely that all the BrdU+ cells colabeled for neuronal progenitor markers were nonneuronal cells.

Two recent studies have demonstrated that endogenous neural progenitors in SVZ are capable of regenerationg neurons in the postischemic rodent striatum (Arvidsson et al., 2002) and CA1 sector (Nakatomi et al., 2002), thus representing an alternative approach for neuronal repair to the transplantation of exogenously propagated neural stem cells. Our results in the monkey show that ischemia increases the generation of neural progenitors severalfold, but induces proliferation only in a limited number of neuronal precursors. Thus, external application of neuronal growth/differentiation factors, as done by Nakatomi et al. (2002), might be indispensable for producing a more significant neuronal regeneration in the primate.

BrdU incorporation by cells with immunophenotype of neuron or glia

The presence of BrdU/NeuN colabeling has been considered as evidence of neurogenesis by previous reports in adult rodents (Liu et al., 1998; Gu et al., 2000; Magavi et al., 2000; Yagita et al., 2001; Arvidsson et al., 2002; Nakatomi et al., 2002) or primates (Eriksson et al., 1998; Gould et al., 1999b; Kornack and Rakic, 1999; Gould et al., 2001). All the primate data reported so far have been restricted to normal brains, in which we did not observe colocalization of BrdU and NeuN or S100β. This difference is probably due to the much shorter lifespan of the BrdU+ cells in our experiments (2–96 h). In the postischemic Days 9 and 15 monkey DG and IT, about 1% of the BrdU+ cells coexpressed NeuN. In the rodent, about 3 and 12% of the BrdU+ cells in DG are costained for the mature neuronal marker calbindin at days 3 and 7, respectively, after global ischemia (Kee et al., 2001). In the rat neocortex at Day 7 after focal ischemic insult, approximately 3% of the proliferating cells are BrdU+/NeuN+ (Gu et al., 2000). Thus, our results are compatible with the findings in rodents.

We found proliferating cells with a neuronal or glial phenotype a long distance away from SVZ within 96 h after the onset of BrdU incorporation. It is unlikely that precursor cells originating in the SVZ can reach the neocortex within this short period of time. A more plausible explanation of our findings is that there are progenitors undergoing cell division outside SVZ. This possibility is also supported by in vivo data in rodents (Gu et al., 2000), and in vitro data in humans (Arsenijevic et al., 2001). Further studies with longer survival times after BrdU may show whether a higher proportion of monkey neural progenitors develops a neuronal fate. Nevertheless, the current results in adult nonhuman primates further highlight the potential of endogenous neuronal precursors in the development of brain-repair strategies. However, our data also implicate that both postischemic progenitor proliferation and maturation in the primate occur to a lower extent than in the rodent.

Experimental methods

Animal operations and BrdU paradigm

All experimental procedures were in accordance with the guidelines of our Institute's Animal Care and Ethics Committee, and the NIH Guide for the Care and Use of Laboratory Animals. Eight female adult (5–9 years of age) Japanese macaques (*Macaca fuscata*) were used: two sham-operated controls and six subjected to ischemia. Ischemia was induced by opening the chest and clipping both the innominate and left subclavian arteries for 20 min under general anesthesia. Body temperature, pupil size, arterial blood pressure, and cerebral blood flow were monitored as reviewed (Yamashima, 2000; Tsukada et al., 2001; Zhao et al., 2002). All monkeys received daily injections of BrdU (100 mg/kg iv; Sigma) for five consecutive days, and were sacrificed 2 h after the last injection (i.e., the age of BrdU-labeled cells in each animal was from 2 to 96 h). The experimental monkeys were euthanized on Days 4 ($n = 2$), 9 ($n = 2$), and 15 ($n = 2$) after ischemia, and the controls on Days 4 and 9 after the sham operation.

Tissue processing

After an anesthetic overdose, the monkeys were intracardially perfused with 4% paraformaldehyde. The brain was removed, tissue blocks were cryoprotected in 30% sucrose and frozen, and 40-μm-thick coronal cryosections were sequentially cut. To reveal incorporated BrdU, DNA was denatured in 50% formamide/2× SSC buffer and 2 N HCl as previously described (Kuhn et al., 1996). Subsequently, the sections were washed in Tris-buffered

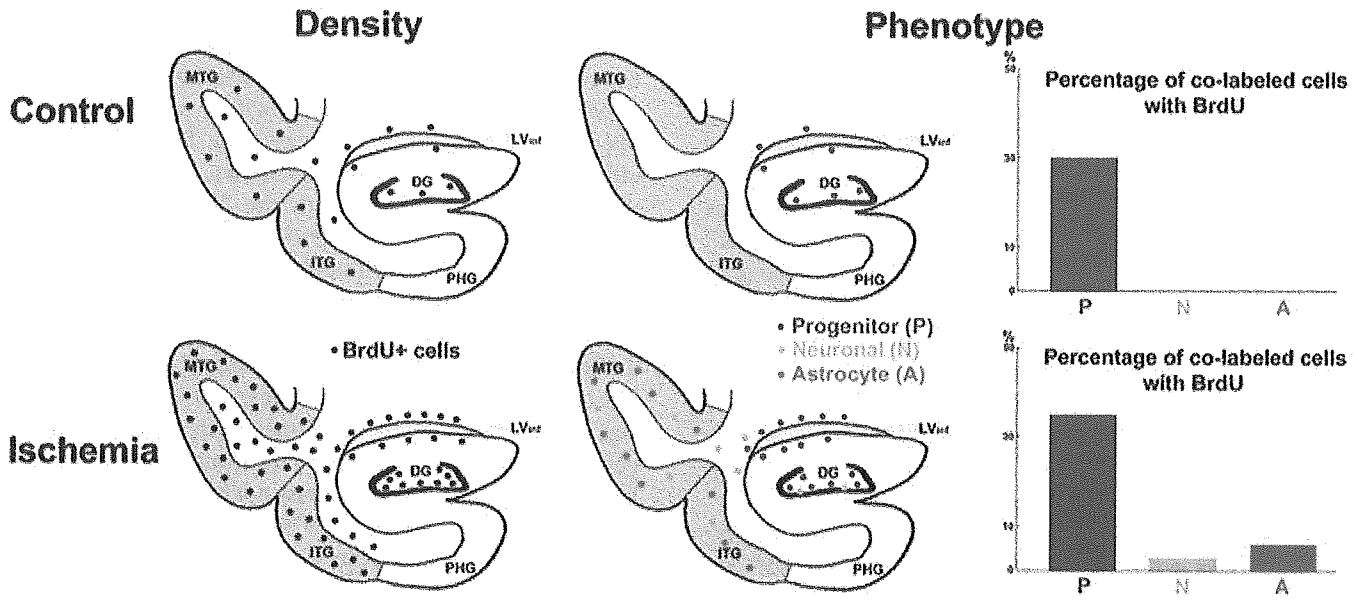

Fig. 4. Schematic summary of findings. A coronal section through the temporal lobe at the level of the hippocampal body. The maps on the left depict positions of BrdU+ cells (black dots) in the denate gyrus (DG), around the walls of the inferior horn of the lateral ventricle (LVinf), and in the inferior and middle temporal gyri (ITG, MTG). The density of dots is indicative of the control and ischemic (Day 9, when proliferation peaked) groups (see Fig. 1W for detailed statistics). The maps on the right show positions of proliferating progenitors (as defined by Musashi1 and Nestin; blue dots), and proliferating cells with neuronal (Hu, βIII-tubulin, doublecortin, TUC4, NeuN; green dots) and astroglial (S100β, GFAP; red dots) immunophenotype. The graphs on the right present average (among the regions of interest in the respective group) percentage of BrdU+ cells colabeled by the corresponding markers. The gray matter of ITG and MTG is indicated in pink. The BrdU+ cells in the hippocampus proper, subiculum, and parahippocampal gyrus (PHG) are omitted for clarity.

saline containing 0.1% Triton X-100 (TBS-T). Nonspecific binding was blocked with TBS-T/10% normal horse or goat sera (TBS-TB) for 30 min, followed by incubation with the primary antibody diluted in TBS-TB for 2 days at 4°C. We used the following primary antibodies and dilutions: mouse anti-BrdU (1:100, Becton-Dickinson, San Jose, CA), rat anti-BrdU (1:100, Harlan Sera-Lab, Loughborough, UK), mouse anti-Ki67 (1:50, Novocastra, Newcastle, UK), rat anti-Musashi1 (1:100; Kaneko et al., 2000), mouse anti-Nestin (1:100; Miyata and Ogawa, 1994), mouse anti-neuronal nuclei (NeuN) (1:100, Chemicon, Temecula, CA), mouse anti-neuronal protein HuC/HuD (anti-Hu) (1:200, Molecular Probes, Eugene, OR), rabbit anti-TUC4 (1:500, Chemicon), mouse anti-β-tubulin class III (1:300, Sigma), rabbit anti-doublecortin (1:500; Mizuguchi et al., 1999), mouse anti-S100β (1:500, Sigma), and rabbit anti-glial fibrillary acid protein (GFAP) (1:200, Sigma).

For peroxidase immunohistochemistry, immunoreactivity was visualized using a Vector ABC kit (Vector Laboratories, Burlingame, CA) with diaminobenzidine (DAB, Sigma) as a chromogen. For fluorescent immunolabeling, primary antibodies were detected using the following goat secondary antibodies/dilutions: anti-rat IgG-TRITC (Jackson Immunoresearch, West Grove, PA), anti-mouse IgG-Alexa Fluor 488 or 546 (Molecular Probes), and anti-rabbit IgG-Alexa Fluor 488 or 633.

Terminal deoxynucleotidyltransferase (TdT)-mediated UTP nick end labeling

The assay was performed on free-floating sections using the ApopTag in situ cell death detection kit (Intergene, Purchase, NY) as described (Bondolfi et al., 2002) with modifications. The sections were washed in TBS-T and then dehydrated in ascending ethanol/dH_2O series (50, 70, and 90%, 5 min each) followed by 15-min incubation in 100% ethanol and rehydration in ethanol/dH_2O (90, 70, and 50%, 5 min each). Then, the sections were equilibrated in proteinase K (PK) reaction buffer (100 mM Tris–HCl, 50 mM EDTA) followed by PK (20 μg/ml, 15 min). PK was washed by several TBS-T rinses before the sections were incubated in equilibration buffer followed by TdT/reaction buffer mixture (15/85, ApopTag kit) at 37°C for 2 h. The reaction was visualized by sheep anti-digoxigenin-fluorescein antibody in blocking solution (62/68, ApopTag kit) overnight at 4°C, followed by anti-sheep-Alexa Fluor 488-conjugated antibody in normal donkey serum for 2 h. DNase pretreatment of the sections prior to the TdT step served as a positive control of the reaction specificity, with TdT omission as a negative control (see Fig. 2P). For TUNEL/NeuN/BrdU triple labeling, the TUNEL assay was performed until the TdT step, then DNA was denatured, followed by digoxigenin visualization. After a positive TUNEL signal was confirmed on the next day, the sections were blocked in

TBS-TB, and BrdU and NeuN were immunostained as described above.

Image acquisition and data analysis

Light microscopic analysis was performed using an Axiovert S100 microscope (Carl Zeiss) connected to a 3CCD digital camera (Fuji). BrdU+ nuclei were counted blindly on every twelfth section per animal and quantified densitometrically (cells/mm^2). In DG and SVZ, the total number of BrdU+ cells was divided by the total area for each section. SGZ and SVZ were defined as 50-μm bands immediately adjacent to the hilar surface of the granule and ependymal cell layers, respectively. In IT (middle and inferior temporal gyri; see Fig. 4), the number of BrdU+ cells was counted separately in the gray and white matter within randomly chosen fields of 880 × 680 μm each. To evaluate neuronal loss in the CA1 sector, NeuN+ cells were counted in 800 × 500 μm frames. Densities were averaged to obtain a mean density value for each sector/animal. No significant difference was observed between the two control monkeys, and the results obtained from them were averaged and are presented together.

Double labeling for BrdU and cell markers was verified using confocal laser scanning microscopy (LSM 510, Carl Zeiss, Tokyo, Japan). Alexa Fluor 488 was appointed in the green channel, TRITC or Alexa Fluor 546 in the red channel, and Alexa Flour 633 in the blue channel. Z sectioning at 0.5-β to 1-μm intervals was performed and optical stacks of at least 10 images were used for analysis. Digital three-dimensional reconstructions were created by the Zeiss LSM software, version 2.3.

Statistics

At least 3000 BrdU+ cells per animal were counted to obtain densities. Data were expressed as means ± SEM. Differences between means were determined by one-way ANOVA followed by Tukey-Kramer's post hoc comparisons for BrdU and two-sided T test for NeuN. Differences were considered significant at $P < 0.05$.

Acknowledgments

Research was supported by grants-in-aid for Strategic Promotion System for Brain Science (SPSBS) from the Japanese Ministry of Education, Culture, Sports, Science and Technology to T.Y., and Japan Science and Technology Corporation (Core Research for Evolutional Science and Technology) to H.O. We thank Drs. Masaharu Ogawa and Takaki Miyata for the gift of anti-Nestin antibody and Dr. Masashi Mizuguchi for providing anti-doublecortin antibody. A.B.T. is also indebted to Drs. George Chaldakov and Masahiko Watanabe for stimulating discussions, and to Dr. Ralica Petrova and Mrs. Kiyoko Wada for technical assistance.

References

Arsenijevic, Y., Villemure, J.G., Brunet, J.F., Bloch, J.J., Deglon, N., Kostic, C., Zurn, A., Aebischer, P., 2001. Isolation of multipotent neural precursors residing in the cortex of the adult human brain. Exp. Neurol. 170, 48–62.

Arvidsson, A., Collin, T., Kirik, D., Kokaia, Z., Lindvall, O., 2002. Neuronal replacement from endogenous precursors in the adult brain after stroke. Nature Med. 8, 963–970.

Bedard, A., Cossette, M., Levesque, M., Parent, A., 2002. Proliferating cells can differentiate into neurons in the striatum of normal adult monkey. Neurosci. Lett. 328, 213–216.

Bernier, P.J., Bedard, A., Vinet, J., Levesque, M., Parent, A., 2002. Newly generated neurons in the amygdala and adjoining cortex of adult primates. Proc. Natl. Acad. Sci. USA 99, 11464–11469.

Bondolfi, L., Calhoun, M., Ermini, F., Kuhn, H.G., Wiederhold, K.H., Walker, L., Staufenbiel, M., Jucker, M., 2002. Amyloid-associated neuron loss and gliogenesis in the neocortex of amyloid precursor protein transgenic mice. J. Neurosci. 22, 515–522.

Cooper-Kuhn, C.M., Kuhn, H.G., 2002. Is it all DNA repair? Methodological considerations for detecting neurogenesis in the adult brain. Brain Res. Dev. Brain Res. 134, 13–21.

Duggal, N., Schmidt-Kastner, R., Hakim, A.M., 1997. Nestin expression in reactive astrocytes following focal cerebral ischemia in rats. Brain Res. 768, 1–9.

Eriksson, P.S., Perfilieva, E., Bjork-Eriksson, T., Alborn, A.M., Nordborg, C., Peterson, D.A., Gage, F.H., 1998. Neurogenesis in the adult human hippocampus. Nature Med. 4, 1313–1317.

Francis, F., Koulakoff, A., Boucher, D., Chafey, P., Schaar, B., Vinet, M.C., Friocourt, G., McDonnell, N., Reiner, O., Kahn, A., McConnell, SK., Berwald-Netter, Y., Denoulet, P., Chelly, J., 1999. Doublecortin is a developmentally regulated, microtubule-associated protein expressed in migrating and differentiating neurons. Neuron 23, 247–256.

Gage, F.H., Kempermann, G., Palmer, T.D., Peterson, D.A., Ray, J., 1998. Multipotent progenitor cells in the adult dentate gyrus. J. Neurobiol. 36, 249–266.

Garcia-Verdugo, J.M., Doetsch, F., Wichterle, H., Lim, D.A., Alvarez-Buylla, A., 1998. Architecture and cell types of the adult subventricular zone: in search of the stem cells. J. Neurobiol. 36, 234–248.

Gleeson, J.G., Lin, P.T., Flanagan, L.A., Walsh, C.A., 1999. Doublecortin is a microtubule-associated protein and is expressed widely by migrating neurons. Neuron 23, 257–271.

Gould, E., Reeves, A.J., Fallah, M., Tanapat, P., Gross, C.G., Fuchs, E., 1999a. Hippocampal neurogenesis in adult Old World primates. Proc. Natl. Acad. Sci. USA 96, 5263–5267.

Gould, E., Reeves, A.J., Graziano, M.S., Gross, C.G., 1999b. Neurogenesis in the neocortex of adult primates. Science 286, 548–552.

Gould, E., Vail, N., Wagers, M., Gross, C.G., 2001. Adult-generated hippocampal and neocortical neurons in macaques have a transient existence. Proc. Natl. Acad. Sci. USA 98, 10910–10917.

Gu, W., Brannstrom, T., Wester, P., 2000. Cortical neurogenesis in adult rats after reversible photothrombotic stroke. J. Cereb. Blood Flow Metab. 20, 1166–1173.

Kaneko, Y., Sakakibara, S., Imai, T., Suzuki, A., Nakamura, Y., Sawamoto, K., Ogawa, Y., Toyama, Y., Miyata, T., Okano, H., 2000. Musashi1: an evolutionally conserved marker for CNS progenitor cells including neural stem cells. Dev. Neurosci. 22, 139–153.

Kee, N.J., Preston, E., Wojtowicz, J.M., 2001. Enhanced neurogenesis after transient global ischemia in the dentate gyrus of the rat. Exp. Brain Res. 136, 313–320.

Kee, N., Sivalingam, S., Boonstra, R., Wojtowicz, J.M., 2002. The utility of Ki-67 and BrdU as proliferative markers of adult neurogenesis. J. Neurosci. Methods 115, 97–105.

Kornack, D.R., Rakic, P., 1999. Continuation of neurogenesis in the hippocampus of the adult macaque monkey. Proc. Natl. Acad. Sci. USA 96, 5768–5773.

Kornack, D.R., Rakic, P., 2001. Cell proliferation without neurogenesis in adult primate neocortex. Science 294, 2127–2130.

Kuhn, H.G., Dickinson-Anson, H., Gage, F.H., 1996. Neurogenesis in the dentate gyrus of the adult rat: age-related decrease of neuronal progenitor proliferation. J. Neurosci. 16, 2027–2033.

Lee, M.K., Rebhun, L.I., Frankfurter, A., 1990. Posttranslational modification of class III β-tubulin. Proc. Natl. Acad. Sci. USA 87, 7195–7199.

Lendahl, U., Zimmerman, L.B., McKay, R.D., 1990. CNS stem cells express a new class of intermediate filament protein. Cell 60, 585–595.

Liu, J., Solway, K., Messing, R.O., Sharp, F.R., 1998. Increased neurogenesis in the dentate gyrus after transient global ischemia in gerbils. J. Neurosci. 18, 7768–7778.

Liu, P.K., Grossman, R.G., Hsu, C.Y., Robertson, C.S., 2001. Ischemic injury and faulty gene transcripts in the brain. Trends Neurosci. 24, 581–588.

Magavi, S.S., Leavitt, B.R., Macklis, J.D., 2000. Induction of neurogenesis in the neocortex of adult mice. Nature 405, 951–955.

Miyata, T., Ogawa, M., 1994. Developmental potentials of early telencephalic neuroepithelial cells: a study with microexplant culture. Dev. Growth Differ. 36, 319–331.

Mizuguchi, M., Qin, J., Yamada, M., Ikeda, K., Takashima, S., 1999. High expression of doublecortin and KIAA0369 protein in fetal brain suggests their specific role in neuronal migration. Am. J. Pathol. 155, 1713–1721.

Mullen, R.J., Buck, C.R., Smith, A.M., 1992. NeuN, a neuronal specific nuclear protein in vertebrates. Development 116, 201–211.

Nacher, J., Rosell, D.R., McEwen, B.S., 2000. Widespread expression of rat collapsin response-mediated protein 4 in the telencephalon and other areas of the adult rat central nervous system. J. Comp. Neurol. 424, 628–639.

Nakatomi, H., Kuriu, T., Okabe, S., Yamamoto, S., Hatano, O., Kawahara, N., Tamura, A., Kirino, T., and Nakafuku, M., 2002. Regeneration of hippocampal pyramidal neurons after ischemic brain injury by recruitment of endogenous neural progenitors. Cell 110, 429–441.

Okano, H.J., Darnell, R.B., 1997. A hierarchy of Hu RNA binding proteins in developing and adult neurons. J. Neurosci. 17, 3024–3037.

Quinn, C.C., Gray, G.E., Hockfield, S., 1999. A family of proteins implicated in axon guidance and outgrowth. J. Neurobiol. 41, 158–164.

Rakic, P., 2002. Adult neurogenesis in mammals: an identity crisis. J. Neurosci. 22, 614–618.

Sakakibara, S., Imai, T., Hamaguchi, K., Okabe, M., Aruga, J., Nakajima, K., Yasutomi, D., Nagata, T., Kurihara, Y., Uesugi, S., Miyata, T., Ogawa, M., Mikoshiba, K., Okano, H., 1996. Mouse-Musashi1, a neural RNA-binding protein highly enriched in the mammalian CNS stem cell. Dev. Biol. 176, 230–242.

Seri, B., Garcia-Verdugo, J.M., McEwen, B.S., Alvarez-Buylla, A., 2001. Astrocytes give rise to new neurons in the adult mammalian hippocampus. J. Neurosci. 21, 7153–7160.

Scholzen, T., Gerdes, J., 2000. The Ki-67 protein: from the known and the unknown. J. Cell Physiol. 182, 311–322.

Takagi, Y., Nozaki, K., Takahashi, J., Yodoi, J., Ishikawa, M., Hashimoto, N., 1999. Proliferation of neuronal precursor cells in the dentate gyrus is accelerated after transient forebrain ischemia in mice. Brain Res. 831, 283–287.

Takasawa, K-I., Kitagawa, K., Yagita, Y., Sasaki, T., Tanaka, S., Ohtsuki, T., Miyata, T., Okano, H., Hori, M., Matsumoto, M., 2002. Increased proliferation of neural progenitor cells but reduced survival of newborn cells in the contralateral hippocampus after focal cerebral ischemia in rats. J. Cereb. Blood Flow Metab. 22, 299–307.

Tsukada, T., Watanabe, M., Yamashima, T., 2001. Implications of CAD and DNase II in ischemic neuronal necrosis specific for the primate hippocampus. J. Neurochem. 79, 1196–1206.

Yagita, Y., Kitagawa, K., Ohtsuki, T., Takasawa, K-I., Miyata, T., Okano, H., Hori, M., Matsumoto, M., 2001. Neurogenesis by progenitor cells in the ischemic adult rat hippocampus. Stroke 32, 1890–1896.

Yamashima, T., 2000. Implication of cysteine proteases calpain, cathepsin and caspase in ischemic neuronal death of primates. Prog. Neurobiol. 62, 273–295.

Zhao, L., Yamashima, T., Wang, X.D., Tonchev, A.B., Yamashita, J., Kakiuchi, T., Nishiyama, S., Kuhara, S., Takahashi, K., Tsukada, H., 2002. PET imaging of ischemic neuronal death in the hippocampus of living monkeys. Hippocampus 12, 109–118.

FEBS 26925

FEBS Letters 535 (2003) 131–135

Candidate markers for stem and early progenitor cells, Musashi-1 and Hes1, are expressed in crypt base columnar cells of mouse small intestine

Takahisa Kayahara[a], Mitsutaka Sawada[a,*], Shigeo Takaishi[a], Hirokazu Fukui[a], Hiroshi Seno[a], Hiroaki Fukuzawa[a], Katsumasa Suzuki[a], Hiroshi Hiai[b], Ryoichiro Kageyama[c], Hideyuki Okano[d], Tsutomu Chiba[a]

[a] *Department of Gastroenterology and Hepatology, Kyoto University Graduate School of Medicine, 54 Shogoin-Kawara-cho, Sakyo-ku, Kyoto 606-8507, Japan*
[b] *Department of Pathology, Kyoto University Graduate School of Medicine, Kyoto, Japan*
[c] *Institute of Virus Research, Kyoto University Graduate School of Medicine, Kyoto, Japan*
[d] *Department of Physiology, Keio University School of Medicine, Tokyo, Japan*

Received 21 November 2002; revised 11 December 2002; accepted 25 December 2002

First published online 8 January 2003

Edited by Masayuki Miyasaka

Abstract Musashi-1, a neural RNA-binding protein, is important for maintaining neural stem cells. Both Musashi-1 and Hes1, a transcriptional factor regulated by Musashi-1, are expressed in the small intestine. Here we show that Musashi-1 is present in a few epithelial cells just above the Paneth cells in the small intestinal crypt, the putative position of stem cells, whereas Hes1 is expressed in lower crypt cells just above the Paneth cells, including Musashi-1-positive cells. Musashi-1 and Hes1 were not expressed in Paneth cells. Notably, Musashi-1 and Hes1 were coexpressed in the crypt base columnar cells located between the Paneth cells. These findings suggest that not only the cells just above Paneth cells but also the crypt base columnar cells between the Paneth cells have stem cell characteristics.

Key words: Musashi-1; Hes1; Small intestine; Stem cell; Crypt base columnar cell

1. Introduction

Small intestinal epithelium is composed of four major cell types: enterocytes, goblet cells, enteroendocrine cells, and Paneth cells. All differentiated epithelial cells in the small intestinal mucosa are believed to originate from multipotent stem cells located just above the crypt base [1–3]. Although recent studies have identified and characterized stem cells in several tissues including the central nervous system [4–6], the stem cells in the small intestinal epithelium have not been well defined, due in part to the lack of good molecular markers for stem cells.

Musashi-1 (Msi-1), a neural RNA-binding protein, has been isolated as a mammalian homologue of a *Drosophila* protein that is required for asymmetric division of sensory neural precursor cells [7,8]. It was subsequently demonstrated that Msi-1 is selectively expressed in neural progenitor cells, including stem cells, and has key roles in the maintenance of the stem cell state and its differentiation [9–12]. Thus, Msi-1 is suggested to be a mammalian neural stem cell marker [4]. On the other hand, recent studies demonstrated that Hes1, a transcriptional factor regulated by Notch signaling [13], is essential for the self-renewing activity of neural stem cells and for repression of their commitment to the neuronal lineage [14–16]. More recently, Imai et al. reported that Msi-1 potentiates *Hes1* promoter activity, suggesting a close link between Msi-1 and Hes1 [17]. And others have reported that both Msi-1 and Hes1 are expressed in the small intestine [4,18]. In the present study, therefore, we investigated Msi-1 and Hes1 expression in the small intestinal epithelial cells of the mouse, and attempted to identify putative stem cells.

2. Materials and methods

2.1. Cell lines and culture

IEC6, originated from rat small intestinal epithelium, and Intestine407, originated from human small intestinal epithelium, were cultured in Dulbecco's modified Eagle's medium supplemented with 2 mM L-glutamine, 100 U/ml penicillin, 100 U/ml streptomycin, and 10% fetal bovine serum at 37°C in a humidified atmosphere containing 5% CO_2. All media and chemicals used in the cell cultures were obtained from Gibco BRL (Grand Island, NY, USA).

2.2. Animals and tissue preparation

ICR mice (Shizuoka Laboratory Animal Center, Shizuoka, Japan) were used in this study. The mice were kept in isolator cages in a barrier facility under a 12 h light cycle and maintained under specific pathogen-free conditions. Postnatal and adult ICR mice were killed at P1, 7, 14, or 21 (day of birth was defined as postnatal day P0). The small intestine was immediately removed and subjected to immunohistochemistry and RNA extraction. All animal procedures followed the guidelines for animal experiments of Kyoto University.

2.3. RNA extraction and reverse transcription-polymerase chain reaction (RT-PCR)

Total RNA was extracted using the single-step guanidinium thiocyanate phenol–chloroform method (Trizol; Gibco BRL). To generate cDNA, 5 μg of total RNA was reverse-transcribed using 200 U of SuperScript II RT (Gibco BRL) in a total reaction volume of 20 μl. For the following PCR, pairs of oligonucleotide primers for mouse *Msi-1*, mouse *Hes1*, and mouse *Glyceraldehyde-3 phosphate dehydrogenase* (*GAPDH*) were prepared: mouse *Msi-1*, 5′-CGAGCTCGACTCCAAAACAAT-3′ (sense) and 5′-GGCTTTCTTGCATTCCACCA-3′ (antisense); mouse *Hes1*, 5′-CTACCCCAGCCAGTGTCAAC-3′ (sense) and 5′-AAGCGGGTCACCTCGTTCAT-3′ (antisense); mouse *GAPDH*, 5′-TTAGCCCCCCTGGCCAAGG-3′ (sense) and

*Corresponding author. Fax: (81)-75-751 4303.
E-mail address: msawada@kuhp.kyoto-u.ac.jp (M. Sawada).

Abbreviations: Msi-1, Musashi-1; GAPDH, glyceraldehyde-3-phosphate dehydrogenase; (RT-)PCR, (reverse transcription-)polymerase chain reaction

0014-5793/03/$22.00
doi:10.1016/S0014-5793(02)03896-6

5′-CTTACTCCTTGGAGGCCATG-3′ (antisense). One microliter of reverse-transcription product was amplified by PCR in a 50 μl reaction volume containing 10 pmol of the above primer sets, 1.25 U Ampli-Taq DNA polymerase (Applied Biosystems, Branchburg, NJ, USA), PCR buffer [final concentration: 20 mM Tris–HCl (pH 8.4), 50 mM KCl], 2.5 mM $MgCl_2$, 10 mM dithiothreitol, and 1 mM dNTP. The PCR amplification was performed as follows: 95°C for 10 min, 40 cycles of 94°C for 30 s, 55°C for 30 s, and 72°C for 1 min, with a final extension step of 72°C for 5 min.

2.4. Immunohistochemistry

The small intestine removed from ICR mice was fixed with 4% paraformaldehyde overnight in 0.1 M phosphate-buffered saline (PBS; pH 7.4) at 4°C, embedded in paraffin and OCT compound (Tissue-Tek; Sakura Finetechnical, Tokyo, Japan), and cut at a thickness of 6 μm. Immunostaining for Msi-1, Hes1, and Ki-67, a proliferation marker, was performed as previously described [10,19]. In brief, sections were treated with 3% H_2O_2 in methanol for 20 min to quench endogenous peroxidase activity. The sections were then placed in 0.01 M citrate buffer (pH 6.0) and treated with microwave heating for 10 min to facilitate antigen retrieval. The sections were immunostained using a Vectastain ABC kit (Vector Laboratories, Burlingame, CA, USA) according to the manufacturer's instructions. Sections were incubated with 3% bovine serum albumin in PBS for 30 min and then incubated with anti-mouse Msi-1 antibody (final dilution 1:1000) [10], anti-mouse Hes1 antibody (kindly supplied by Dr. T. Sudo, Toray Industries, Tokyo, Japan, final dilution 1:1000) [19], or anti-mouse Ki-67 antibody (Dako Cytomation, Copenhagen, Denmark; final dilution 1:200, according to the manufacturer's instructions) at 37°C for 30 min. The sections were incubated with biotinylated secondary antibody for 40 min. After washing with PBS, avidin–biotin complex was applied for 30 min. The sections were then incubated in 3,3′-diaminobenzidine tetrahydrochloride with 0.05% H_2O_2 for 3 min and counterstained with Mayer's hematoxylin.

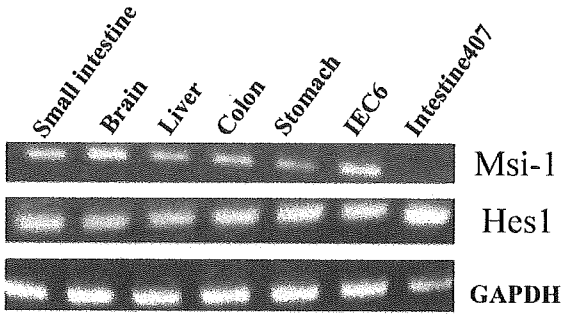

Fig. 1. RT-PCR analysis of *Msi-1* and *Hes1* mRNA expression in mouse normal tissues, IEC6, and Intestine407 cell lines. *Msi-1* and *Hes1* expression was detected in all tissues examined and IEC6. *Hes1* was expressed in Intestine407. *GAPDH* expression is shown as internal control.

3. Results

3.1. Expression of Msi-1 and Hes1 mRNAs in adult mouse tissue and intestinal cell lines

The PCR-amplified products obtained using Msi-1-specific and Hes1-specific primers had clear bands of the predicted sizes, 304 bp and 322 bp, respectively. The PCR product sequence was confirmed using the dideoxy chain termination procedure. *Msi-1* mRNA expression was detected in small intestine, colon, stomach, liver, and IEC6. *Msi-1* mRNA expression was not detected in Intestine407. On the other hand,

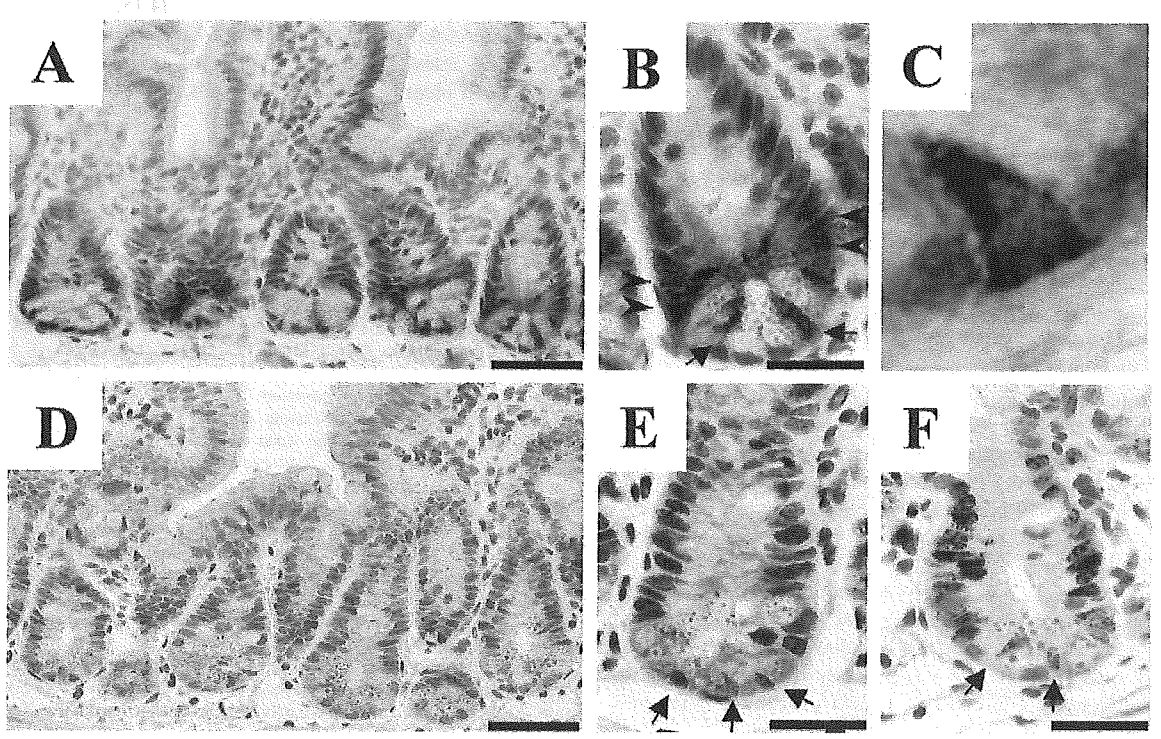

Fig. 2. Immunohistochemical analysis of Msi-1 (A–C), Hes1 (D,E), and Ki-67 (F) in adult mouse small intestine. A few crypt cells just above the Paneth cells (arrowhead) and the crypt base columnar cells between the Paneth cells (arrow) were stained with Msi-1 antibody. Msi-1 was absent in the Paneth cells. No Msi-1-positive cells were detected at the villous epithelium (A,B). Higher magnification of a crypt base columnar cell. Msi-1 reactivity was located in the cytoplasm, and the cell nucleus was not stained (C). Hes1 was predominantly expressed in mid to lower crypt cell nuclei and immunoreactivity gradually increased toward the crypt base. Goblet and Paneth cell nuclei were not stained. Crypt base columnar cells were also stained with Hes1 antibody (arrow) (D,E). Mid to basal part of crypt epithelial cells were stained with Ki-67 antibody. Moreover, crypt base columnar cells were also positive for Ki-67 (arrow) (F). Bars indicate 50 μm (B,E,F), and 100 μm (A,D).

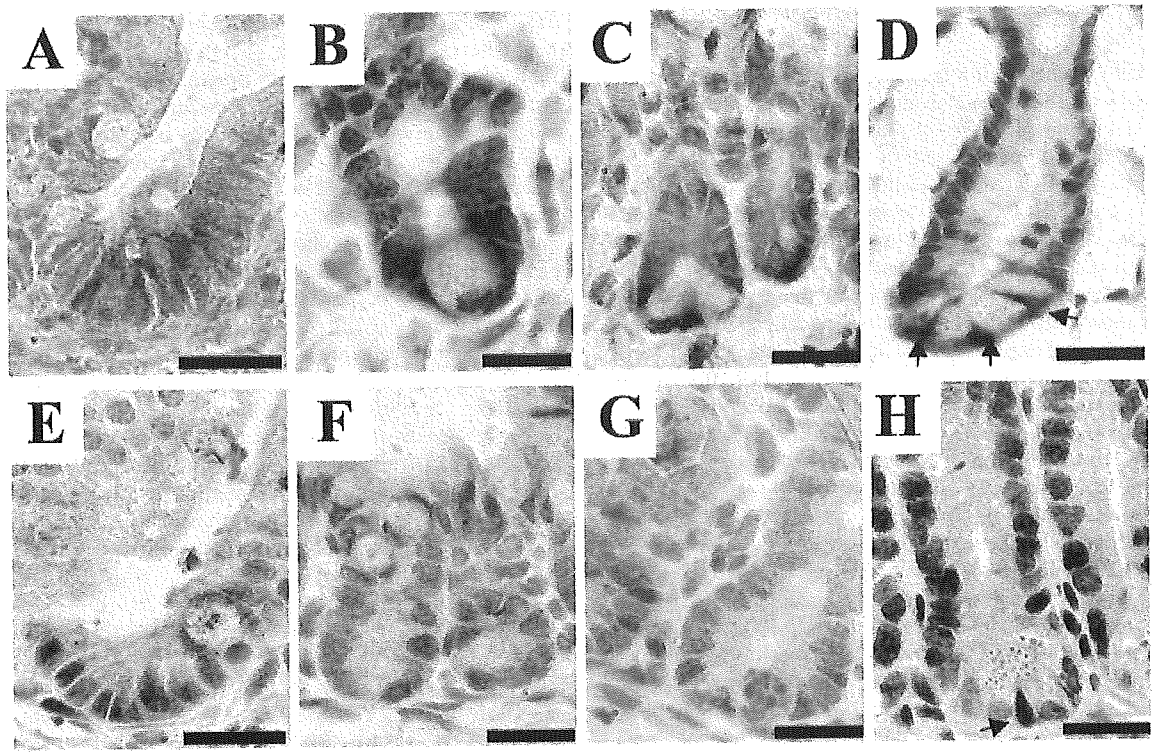

Fig. 3. Expressions of Msi-1 (A–D) and Hes1 (E–H) protein during the development of mouse small intestine. In P1 mice, there were no crypt structures. Both Msi-1 and Hes1 were detected in the intervillus epithelial cells (A,E). In P7 mice, small crypt structures were observed in the intervillus space and single Paneth cell began to appear in the crypt base. Almost all crypt cells were stained by both Msi-1 and Hes1 antibodies, but not the Paneth cells (B,F). In P14 mice, Msi-1 was expressed at the lower part of the single crypt. Msi-1 was not expressed in the Paneth cells (C). On the other hand, Hes1 was also expressed in the crypt cells, and the cells adjacent to the Paneth cells had strong reactivity to the Hes1 antibody (G). Two or three Paneth cells were observed in the intestinal crypt of P21 mice (D,H). In addition to the cells just above the Paneth cells, the crypt base columnar cells between Paneth cells were stained with both Msi-1 (D) and Hes1 (H) antibodies (arrow). Bars indicate 50 μm.

Hes1 mRNA expression was detected in all samples examined (Fig. 1).

3.2. *Msi-1 and Hes1 protein expression in adult mouse small intestine*

In adult mouse small intestine, Msi-1 expression was observed in a few cells just above the Paneth cells. The Msi-1-positive cells were located where the stem cells are thought to be located [1–3,20–22]. In contrast, Paneth cells were completely devoid of Msi-1 immunoreactivity. In addition to those Msi-1-positive cells just above the Paneth cells, crypt base columnar cells located between the Paneth cells were stained with the anti-mouse Msi-1 antibody. On the other hand, Msi-1 immunoreactivity was not detected in villus structures or the upper part of the crypt (Fig. 2A–C).

Hes1 was expressed in the nuclei of the cells at the lower part of the crypt including Msi-1-positive cells just above Paneth cells, but not in the goblet or Paneth cells. In the crypt–villus axis, Hes1 immunoreactivity was most prominent in the cells just above the Paneth cells and gradually decreased toward the villus tip. Of note, the nuclei of Msi-1-positive crypt base columnar cells between Paneth cells were also strongly positive for Hes1 (Fig. 2D,E). In addition to a few cells just above the Paneth cells, crypt base columnar cells between the Paneth cells were also positive for Ki-67 staining (Fig. 2F).

3.3. *Expression of Msi-1 and Hes1 protein during the development of mouse small intestine*

There was no crypt formation in mouse small intestine at P1. At P1, both Msi-1 and Hes1 expression were detected in the cells located at the intervillus region (Fig. 3A,E). Incomplete crypts were observed at P7, and a single Paneth cell appeared in some of those crypts. Expression of both Msi-1 and Hes1 was detected in a few cells adjacent to the Paneth cells in the crypt base, whereas Msi-1 and Hes1 immunoreactivity was completely absent in the Paneth cells (Fig. 3B,F). From P7 to P14, crypts became longer and some crypts became bifurcated. Msi-1 and Hes1 expression were still observed in the cells adjacent to the Paneth cells (Fig. 3C,G). Morphologically, crypt formation was almost complete at P21 and more than two Paneth cells were observed in each crypt base. Hes1-positive cells localized at the lower to middle portion of the crypts and further increased in number from P14. A few Msi-1-positive cells were localized just above the Paneth cells and thus their distribution was more restricted than that of Hes1. In addition, the crypt base columnar cells began to appear between the Paneth cells, and were immunoreactive for both Msi-1 and Hes1 (Fig. 3D,H) on P21. Villus enterocytes, goblet cells, and Paneth cells were not immunoreactive for Msi-1 or Hes1 throughout the developmental period.

4. Discussion

Stem cells of the small intestinal epithelium are believed to be located just above the Paneth cells in the crypt base, and migrate both upward toward the lumen of the gut and downward toward the crypt base as they mature [1–3,23,24]. In the present study, cells at the intervillus region were stained for both Msi-1 and Hes1 in the developmental period. But, in adult mice, Msi-1 was expressed in only a few cells just above the Paneth cells of the small intestinal crypt, and Hes1 was present in the cells at the lower part of the crypt, including Msi-1-positive cells. Msi-1 is present specifically in neural stem cells, and has an important role in the maintenance of the neural stem cell state and its differentiation [4,9,10]. Moreover, recent studies demonstrated that Hes1 is positively regulated by Msi-1, and is involved in neural stem cell self-renewal [17]. Thus, co-localization of Msi-1 and Hes1 in the cells just above the Paneth cells in adult mice strongly suggests that these cells represent progenitor cells, or stem cells of the small intestinal mucosa, supporting the concepts reported previously [1–3,21]. Furthermore, an attractive hypothesis derived from the present study is that Notch signaling plays an important role in the maintenance of the intestinal stem cells. However, it may also be noted that Hes1-positive cells were more broadly distributed than Msi-1-positive cells. Thus, it may be considered that although Hes1 and Msi-1 double positive cells represent stem cells, most Hes1-positive cells are transit-amplifying cells of the crypt and villous epithelial cell lineage.

Another interesting finding of the present study is that in addition to the cells just above the Paneth cells, crypt base columnar cells located between Paneth cells were also strongly positive for both Msi-1 and Hes1, while Paneth cells themselves were completely devoid of Msi-1 and Hes1 immunoreactivity. Furthermore, the Msi-1- and Hes1-positive cells just above and between the Paneth cells were both positive for Ki-67, indicating their high proliferative activity. These data suggest that crypt base columnar cells also have stem cell-like characteristics. Previously, Cheng et al. reported electron microscopic observations that the labeling of crypt base columnar cells after injection of [^{3}H]thymidine was followed by the labeling of Paneth cells, and suggested that Paneth cells originate from crypt base columnar cells [20,25,26]. Our present data might support this hypothesis. Furthermore, a recent report showed that crypt base columnar cells have a similar expression profile of EphB/EprinB to that of stem cells, which is distinct from Paneth cells [27].

In this study, we found that in addition to Hes1 single positive cells, Msi-1 and Hes1 double positive cells just above and between Paneth cells were both positive for Ki-67, indicating their high proliferating activity. Furthermore, we found that those Msi-1 and Hes1 double positive cells were also positive for bromodeoxyuridine (data not shown). It appears that most Ki-67-positive cells that have only Hes1 but not Msi-1 expression are transit-amplifying cells. However, since stem cells are believed to be in a dormant state generally, the reason why Msi-1 and Hes1 double positive putative stem cells expressed Ki-67 in our study needs to be clarified in a future study.

It has been believed that all the differentiated epithelial cells in the small intestinal mucosa, including Paneth cells, originate from common pluripotent stem cells located just above the Paneth cells [1–3], and that crypt base columnar cells might be transit cells in the Paneth cell lineage rather than stem cells [28]. However, the present study clearly demonstrated that not only the cells just above the Paneth cells but also the crypt base columnar cells were positive for both Msi-1 and Hes1. Thus, although it is not clear at present whether the Msi-1 and Hes1 double positive cells just above the Paneth cells and those located between the Paneth cells represent distinct progenitor cells of different cell lineage, it is possible that the cells just above the Paneth cells are the progenitor cells for crypt cells and villous epithelial cells that migrate toward the villus tip, while crypt base columnar cells between Paneth cells are the progenitor cells for only Paneth cells. In this regard, it may be noted that although both Msi-1 and Hes1 are absent in Paneth cells, Msi-1 disappears but Hes1 remains in the epithelial cells of the lower crypt just above the Msi-1 and Hes1 double positive putative stem cells. Thus, the mechanism of differentiation involving Msi-1 and Hes1 might be different between the putative stem cells just above the Paneth cells and those located between the Paneth cells.

Acknowledgements: We are grateful to Mr. Haruyasu Kohda for his technical assistance with the immunohistochemistry. This experiment was supported by Grants-in-Aid for Scientific Research from the Ministry of Culture and Science of Japan (11470130, 11877090, 11670496, and 13670510) and a Grant-in-Aid for Research for the Future Program from the Japan Society for the Promotion of Science (JSPS-RFTF 97100201).

References

[1] Cheng, H. and Leblond, C.P. (1974) Am. J. Anat. 141, 537–561.
[2] Bjerknes, M. and Cheng, H. (1981) Am. J. Anat. 160, 51–63.
[3] Booth, C. and Potten, C.S. (2000) J. Clin. Invest. 105, 1493–1499.
[4] Sakakibara, S., Imai, T., Hamaguchi, K., Okabe, M., Aruga, J., Nakajima, K., Yasutomi, D., Nagata, T., Kurihara, Y., Uesugi, S., Miyata, T., Ogawa, M., Mikoshiba, K. and Okano, H. (1996) Dev. Biol. 176, 230–242.
[5] Spangrude, G.J., Smith, L., Uchida, N., Ikuta, K., Heimfeld, S., Friedman, J. and Weissman, I.L. (1991) Blood 78, 1395–1402.
[6] Schultz, E. and McCormick, K.M. (1994) Rev. Physiol. Biochem. Pharmacol. 123, 213–257.
[7] Nakamura, M., Okano, H., Blendy, J.A. and Montell, C. (1994) Neuron 13, 67–81.
[8] Okabe, M., Imai, T., Kurusu, M. and Hiromi, Y. (2001) Nature 411, 94–98.
[9] Sakakibara, S. and Okano, H. (1997) J. Neurosci. 17, 8300–8312.
[10] Kaneko, Y., Sakakibara, S., Imai, T., Suzuki, A., Nakamura, Y., Sawamoto, K., Ogawa, Y., Miyata, T. and Okano, H. (2000) Dev. Neurosci. 22, 139–153.
[11] Okano, H., Imai, T. and Okabe, M. (2002) J. Cell Sci. 115, 1355–1359.
[12] Sakakibara, S., Nakamura, Y., Yoshida, T., Shibata, S., Koike, M., Takano, H., Ueda, S., Uchiyama, Y., Noda, T. and Okano, H. (2002) Proc. Natl. Acad. Sci. USA 99, 15194–15199.
[13] Jarriault, S., Brou, C., Logeat, F., Schroeter, E.H., Kopan, R. and Israel, A. (1995) Nature 377, 355–358.
[14] Akazawa, C., Sasai, Y., Nakanishi, S. and Kageyama, R. (1992) J. Biol. Chem. 267, 21879–21885.
[15] Sasai, Y., Kageyama, R., Tagawa, Y., Shigemoto, R. and Nakanishi, S. (1992) Genes Dev. 6, 2620–2634.
[16] Nakamura, Y., Sakakibara, S., Miyata, T., Ogawa, M., Shimazaki, T., Weiss, S., Kageyama, R. and Okano, H. (2000) J. Neurosci. 20, 283–293.
[17] Imai, T., Tokunaga, A., Yoshida, T., Hashimoto, M., Mikoshiba, K., Weinmaster, G., Nakafuku, M. and Okano, H. (2001) Mol. Cell. Biol. 21, 3888–3900.
[18] Jensen, J., Pedersen, E.E., Galante, P., Hald, J., Heller, R.S.,

Ishibashi, M., Kageyama, R., Guillemot, F., Serup, P. and Madsen, O.D. (2000) Nat. Genet. 24, 36–44.
[19] Ito, T., Udaka, N., Yazawa, T., Okudera, K., Hayashi, H., Sudo, T., Guillemot, F., Kageyama, R. and Kitamura, H. (2000) Development 127, 3913–3921.
[20] Cheng, H. (1974) Am. J. Anat. 141, 521–535.
[21] Cheng, H., Merzel, J. and Leblond, C.P. (1969) Am. J. Anat. 126, 507–525.
[22] Potten, C.S., Booth, C., Tudor, G.L., Booth, D., Brady, G., Hurley, P., Ashton, G., Clarke, G., Sakakibara, S. and Okano, H. (2003) Differentiation 7, 28–41.
[23] Sawada, M., Takahashi, K., Sawada, S. and Midorikawa, O. (1991) Int. J. Exp. Pathol. 72, 407–421.
[24] Sawada, M., Nishikawa, M., Adachi, T., Midorikawa, O. and Hiai, H. (1993) Lab. Invest. 68, 338–344.
[25] Benke, O. and Moe, H. (1964) J. Cell Biol. 22, 633–652.
[26] Hampton, J.C. (1968) Cell Tissue Kinet. 1, 309–317.
[27] Batlle, E., Henderson, J.T., Beghtel, H., van den Born, M.M., Sancho, E., Huls, G., Meeldijk, J., Robertson, J., van de Wetering, M., Pawson, T. and Clevers, H. (2002) Cell 111, 251–263.
[28] Chwalinski, S. and Potten, C.S. (1989) Am. J. Anat. 186, 397–406.

Journal of Neuroscience Research 72:461–471 (2003)

Implication of Cyclooxygenase-2 on Enhanced Proliferation of Neural Progenitor Cells in the Adult Mouse Hippocampus After Ischemia

Tsutomu Sasaki,[1]* Kazuo Kitagawa,[1] Shiro Sugiura,[1] Emi Omura-Matsuoka,[1] Shigeru Tanaka,[1] Yoshiki Yagita,[1] Hideyuki Okano,[3] Masayasu Matsumoto,[2] and Masatsugu Hori[1]

[1]Division of Strokology, Department of Internal Medicine and Therapeutics, Osaka University Graduate School of Medicine, Osaka, Japan
[2]Department of Clinical Neuroscience and Therapeutics, Division of Integrated Medical Science Programs for Biomedical Research, Hiroshima University Graduate School of Biomedical Sciences, Hiroshima, Japan
[3]Department of Physiology, Keio University Graduate School of Medicine, Tokyo, Japan

Global ischemia promotes neurogenesis in the dentate gyrus of the adult mouse hippocampus. Cyclooxygenase (COX)-2, the principal isoenzyme in the brain, modulates inflammation, glutamate-mediated cytotoxicity, and synaptic plasticity. We demonstrated that delayed treatment with different classes of COX inhibitor significantly blunted enhancement of dentate gyrus proliferation of neural progenitor cells after ischemia. COX-2 immunoreactivity was observed in both neurons and astrocytes in the dentate gyrus, but not in neural progenitor cells in the subgranular zone. Moreover, in the postischemic dentate gyrus of heterozygous and homozygous COX-2 knockout mice, proliferating bromodeoxyuridine-positive cells were significantly fewer than in wild-type littermates. These results demonstrate that COX-2 is an important modulator in enhancement of proliferation of neural progenitor cells after ischemia.

Key words: neurogenesis; hippocampus; COX-2; neuronal progenitor; musashi-1

In the subgranular zone (SGZ) of the dentate gyrus of the hippocampus and subventricular zone (SVZ) of the lateral ventricles, progenitor cells generate new neurons throughout adulthood. Ischemic insults to the brain have been shown to promote hippocampal neurogenesis in adult gerbils and rats (Liu et al., 1998; Jin et al., 2001; Yagita et al., 2001; Zhang et al., 2001; Iwai et al., 2002; Takasawa et al., 2002). Although, fibroblast growth factor-2 (FGF-2) and glutamate have been proposed to be involved in hippocampal neurogenesis after ischemia (Bernabeu and Sharp, 2000; Arvidsson et al., 2001; Yoshimura et al., 2001; Nakatomi et al., 2002), the molecular and cellular mechanisms underlying postischemic enhancement of neurogenesis remain unclear.

Cyclooxygenase (COX), a rate-limiting enzyme in synthesis of prostaglandins (PGs) from arachidonic acid, produces PGH2, which in subsequent steps gives rise to PGs with varied physiologic functions (Hayaishi, 1991; Smith et al., 1996; Kaufmann et al., 1997). Two Cox isoenzymes exist, COX-1 and COX-2, and COX-2 is expressed constitutively at relatively high levels in brain and kidney (Yamagata et al., 1993). In addition to the role of COX-2 in proinflammatory actions in the central nervous system (CNS), recent studies have found COX-2 to be a multifunctional neural modulator affecting synaptic plasticity (Kaufmann et al., 1996; Bazan, 2001) and glutamate-mediated cytotoxicity (Nogawa et al., 1997; Iadecola et al., 2001b). COX-2 also acts importantly in cell proliferation and has been implicated in growth and progression of a variety of tumor types (Tsujii et al., 1998; Shono et al., 2001).

Evidence is accumulating that quantities of circulating adrenal steroids negatively regulate neurogenesis in the dentate gyrus throughout life (Cameron and Gould, 1994; Gould and Cameron, 1996; Cameron and McKay, 1999) Glucocorticoids selectively inhibit expression of COX-2 without affecting COX-1. Thus, to determine whether COX-2 influences hippocampal neurogenesis in adult mice, we examined postischemic proliferation of progenitor cells in the SGZ after administering COX inhibitors with various specificities and postischemic neurogenesis in

Contract grant sponsor: Grant-in-aid for Scientific Research in Japan; Contract grant sponsor: The Takeda Science Foundation.

*Correspondence to: Tsutomu Sasaki, Division of Strokology, Department of Internal Medicine and Therapeutics (A8), Osaka University Graduate School of Medicine, 2-2 Yamadaoka, Suita City, Osaka 565-0871, Japan. E-mail: sasaki@medone.med.osaka-u.ac.jp

Received 22 October 2002; Revised 8 January 2003; Accepted 24 January 2003

COX-2 knockout mice. Because only a few experimental studies have examined neurogenesis in forebrain ischemia (Takagi et al., 1999) and focal ischemia (Yoshimura et al., 2001) in mice, we established initially profiles of hippocampal neurogenesis after ischemic insults to the mouse forebrain (Kitagawa et al., 1998).

MATERIALS AND METHODS

Animals

Adult male C57Black/6 mice (11–12 weeks old) were used in this study. The experimental protocol was approved by the Institutional Animal Care and Use Committee of Osaka University Graduate School of Medicine. They were fed standard laboratory chow and had free access to water before and after all procedures. Animal care was given according to the guidelines of Animal Center of Osaka University Graduate School of Medicine.

Cyclooxygenase-2 knockout mice (Dinchuk et al., 1995) were obtained from Jackson laboratories (Bar Harbor, ME). Mice were backcrossed to C57Black/6 mice five to seven times, and were studied at age of 10–12 weeks. Experiments were carried out in age-matched littermates, including those homozygous for the knockout (−/−), heterozygous (+/−), and wild type (+/+). Genotypes of all COX-2 knockout mice were determined by PCR analysis.

Transient Forebrain Ischemia

General anesthesia was maintained with 1% halothane by means of an open facemask. A polyacrylamide column for measurement of cortical microperfusion by laser-Doppler flowmetry (LDF; Advanced Laser Flowmetry) was attached to the skull, 3 mm lateral to the bregma on the right side, with dental cement. Body and skull temperature were monitored and maintained at 36.5–37.5°C with a heat lamp and mat. Both common carotid arteries were occluded for 12 min with microaneurysm clips and then reperfused. As described previously, only mice that showed less than 13% of baseline control microperfusion during the first minute of occlusion were used in subsequent experiments (Kitagawa et al., 1998).

Bromodeoxyuridine Labeling Protocols

Bromodeoxyuridine (BrdU; Roche Diagnostics, Indianapolis, IN), a thymidine analogue, was used to label proliferating cells. In the first experiment, mice with no surgery (control), mice with sham ischemia, and mice with ischemia were injected intraperitoneally (i.p.) with BrdU (50 mg/kg) four times every 2 hr over 6 hr to conclude at 6 hr, or 3, 6, 9, 13, and 27 days after ischemia. The next day, mice were killed under deep pentobarbital anesthesia and their brains were immersion-fixed in methanol at 4°C overnight for quantification of BrdU-positive cells. In other mice, to evaluate the phenotype of postmitotic cells, we injected BrdU (50 mg/kg) i.p. 9 days after ischemia four times every 2 hr over 6 hr. These mice were killed at 1, 14, or 30 days after BrdU administration. Mice with no surgery underwent the same sequence of injections and were sacrificed at corresponding times as a control group. Mice were perfused transcardially with 4% paraformaldehyde (PFA), then brains were removed and fixed in 4% PFA at 4°C overnight.

In the second experiment, examining the effect of COX in cell proliferation after ischemia, both right and left common carotid arteries were occluded for 12 min as described above. Ischemic mice were divided randomly into three groups. Indomethacin (Cayman Chemical, Ann Arbor, MI; 10 mg/kg), NS-398, (Cayman Chemical; 20 mg/kg), or vehicle alone was given at 9:00 AM and 9:00 PM on Day 8, and at 9:00 AM on Day 9 after ischemia. NS-398 inhibits COX-2 1,000 times more potently than COX-1 (Masferrer et al., 1994; Reitz et al., 1994). We administered BrdU (50 mg/kg) i.p. four times every 2 hr for 6 hr, starting 2 hr after the last injection of each COX inhibitor.

In the third experiment, we subjected COX-2 knockout mice, including homozygous (−/−), heterozygous (+/−), and wild-type littermates, to ischemia and BrdU-labeling protocols above.

Immunohistochemistry

For quantification of BrdU-positive cells, each tissue block was dehydrated after fixation and embedded in paraffin. Tissue sections (4 μm) encompassing the dorsal hippocampus 1.9 mm caudal from the bregma were examined after staining with cresyl violet. The protocol of BrdU immunohistochemistry was described previously (Takasawa et al., 2002). In brief, each deparaffinized section was treated in 50% formamide and 2× saline-sodium citrate buffer (2× SSC), and then incubated in 2 N HCl. After washing, sections were incubated with a rat monoclonal anti-BrdU antibody, 1:100 (Harlan Sera-Labo, Loughborough, UK) at 4°C overnight. Sections were then washed, incubated with a biotinylated secondary antibody, washed, and incubated further with a streptavidin-biotin-peroxidase complex (Vector Laboratories, Burlingame, CA). The sections were reacted finally with 0.05% 3′3-diaminobenzidine in the presence of 0.01% H_2O_2.

For double immunofluorescence, free-floating sections (40 μm) were incubated with primary antibody diluted with TBS/0.1% Triton X-100 containing 1.5% normal serum at 4°C overnight. Other mice were used for examination with frozen sections to assess COX-2 immunoreactivity. The following primary antibodies were used for immunofluorescence; rat monoclonal anti-BrdU antibody, 1:100 (Harlan Sera-Labo); mouse monoclonal anti-BrdU antibody, 1:200 (Amersham, Piscataway, NJ); mouse monoclonal anti-NeuN antibody, 1:200 (Chemicon, Temecula, CA); mouse monoclonal anti-microtubule associated protein (MAP) 2 antibody, 1:100 (Sigma, St. Louis, MO); rabbit polyclonal anti-glial fibrillary acidic protein (GFAP) antibody, 1:200 (Sigma); mouse monoclonal anti-glial fibrillary acidic protein (GFAP) antibody, 1:200 (Sigma); goat polyclonal anti-doublecortin (DCX) antibody, 1:100 (Santa Cruz Biotechnology, Santa Cruz, CA); rat monoclonal anti-Musashi-1 (Msi-1) antibody (14H1) (Kaneko et al., 2000) 1:200; mouse monoclonal anti-β-tubulin III antibody, 1:200 (Chemicon); and rabbit polyclonal anti-COX-2 antibody, 1:200 (Cayman Chemical).

For double labeling of BrdU and cell markers (NeuN and MAP2 for mature neurons, β-tubulin III for immature neurons, GFAP for astrocytes, DCX for migrating neuroblasts and immature neurons, and Msi-1 for neuronal progenitors, neuronal stem cells, and astrocytes), sections were incubated with an anti-BrdU antibody plus an antibody for one of the above cell

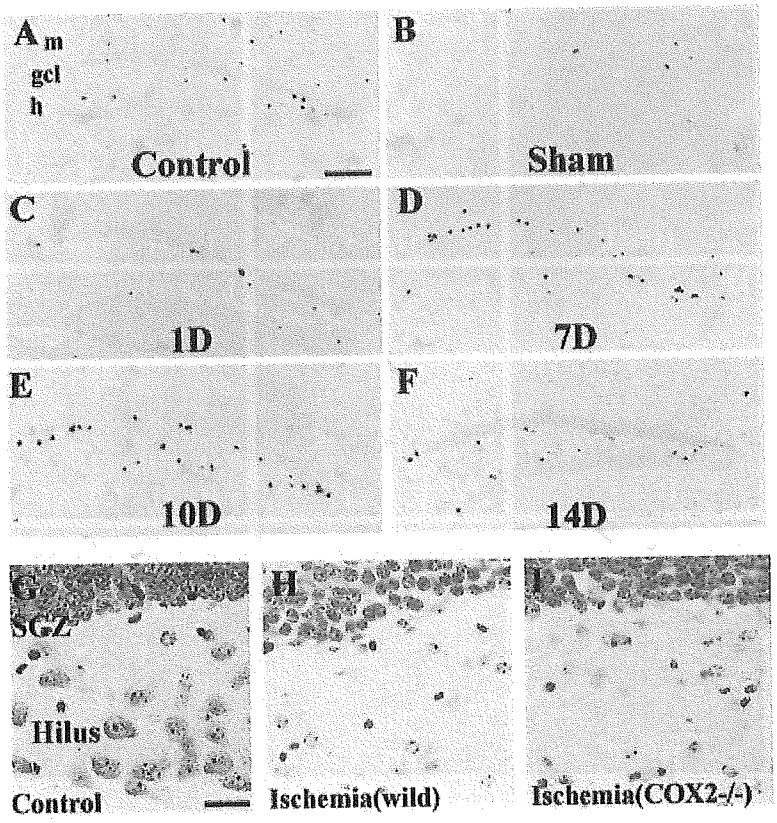

Fig. 1. Distribution of BrdU-positive cells in the mouse dentate gyrus after forebrain ischemia. BrdU (50 mg/kg, i.p.) was administered four times every 2 hr over 6 hr. Mice received BrdU concluding at 6 hr or 3, 6, 9, 13, or 27 days after ischemia ($n = 6$ in each group). On the next day mice were killed, and brains were processed for BrdU immunohistochemistry. Ischemia resulted in an increase of BrdU-positive proliferating cells in the subgranular zone (SGZ). Control (**A**), nonischemic sham (**B**), and ischemic mice killed 1 (**C**), 7 (**D**), 10 (**E**), and 14 (**F**) after ischemia. Neuronal damage was assessed histologically by Nissl staining (**G–I**). COX-2 knockout mice (I) showed a similar degree of neuronal loss in the dentate hilus as in wild-type littermates (H). Scale bars = 0.1 mm in A (applies to A–F); 50 μm in G (applies to G–I). [Color figure can be viewed in the online issue, which is available at www.interscience.wiley.com.]

markers at 4°C overnight after DNA denaturation, and then incubated with appropriate anti-IgG secondary donkey antibodies conjugated to fluorescein isothiocyanate (FITC) or rhodamine (Chemicon, 1:200) for 90 min at room temperature. After rinsing with Tris buffer, sections were mounted with Vectorshield (Vector Laboratories) and visualized or photographed with a confocal microscopy system (Zeiss LSM-410, Oberkochen, Germany).

Quantification

To count BrdU-labeled cells as identified by the immunoperoxidase reaction, five sections from the hippocampus were cut every 120 μm beginning 1.4 mm caudal and 1.9 mm caudal to the bregma. In the hippocampus, the granular cell layer (GCL, 50 μm) and SGZ, defined as a zone two cell bodies wide (5 μm) along the border of the GCL and hilus, were considered together for quantification. The mean density of BrdU-labeled cells in each mouse was calculated as the number of labeled nuclei divided by the area.

To assess the phenotype of BrdU-labeled cells after ischemia or sham ischemia in double immunofluorescence, we detected BrdU-positive cells in the SGZ and GCL, and then determined whether these cells expressed Msi-1, DCX, β-tubulin III, NeuN, MAP2, or GFAP. A mean value for each marker was obtained using 10 sections from five mice. Data in the text and figure are described as mean ± SD. Multiple comparisons were evaluated statistically by the analysis of variance, followed by Scheffe's post-hoc tests.

RESULTS

Cell Proliferation in the Mouse Hippocampus After Ischemia

A few BrdU-positive cells were observed in the SGZ of the hippocampal dentate gyrus in the control (Fig. 1A; 21.6 ± 10.7/mm^2, $n = 10$). The temporal and regional profiles of BrdU labeling in the SGZ did not differ significantly between nonischemic control mice and mice with sham ischemia (Fig. 1B; 18.9 ± 10.2/mm^2, $n = 6$). BrdU-positive cells exhibited a slight decrease 1 day after the ischemic insult (Fig. 1C; 11.2 ± 8.0/mm^2, $n = 6$). The number of BrdU-positive cells in the SGZ was increased at 4 days (51.5 ± 21.9/mm^2, $n = 6$), reached a peak at 7 and 10 days (Fig. 1D; 77.0 ± 33.3/mm^2, $n = 6$ and Fig. 1E; 98.7 ± 26.6/mm^2, $n = 6$, respectively), then declined by 14 days (Fig. 1F; 45.5 ± 22.1/mm^2, $n = 6$), and returned to the control levels by 28 days (20.4 ± 11.1/mm^2, $n = 6$) after ischemia. Semiquantitative analysis in the SGZ showed the number of BrdU-positive cells to be increased significantly compared to the control and sham groups by 4–5 times at 7 and 10 days after ischemia.

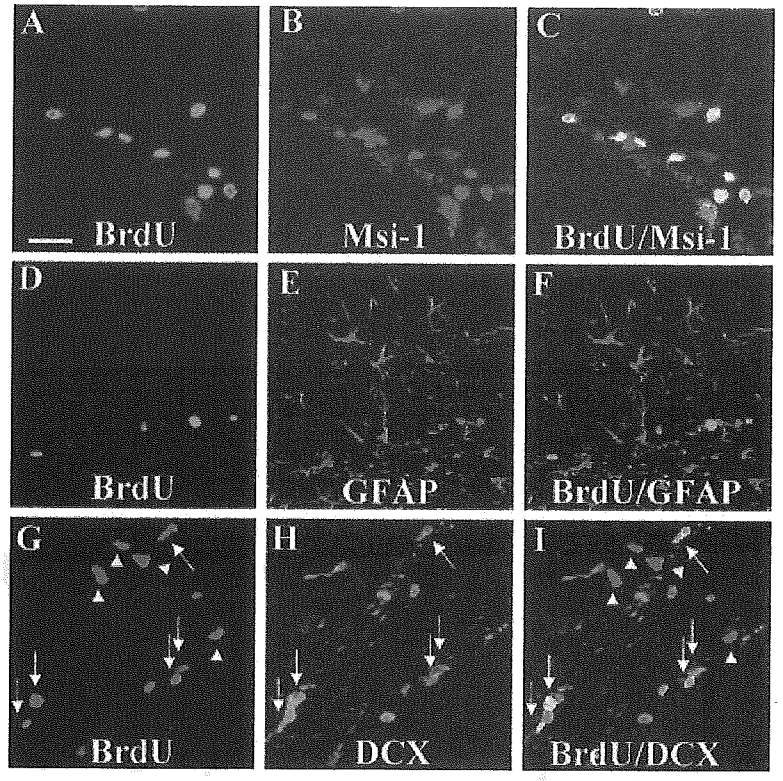

Fig. 2. Characterization of newly generated cells in the SGZ and GCL. To label new cells, mice received BrdU (50 mg/kg, i.p. administration) four times on Day 9 after ischemia. In the SGZ and GCL, double immunofluorescent staining shows BrdU-immunoreactive cells (**A**, **D**, **G**), and cells immunoreactive for Msi-1 (**B**), GFAP (**E**), or DCX (**H**). Merged images show BrdU/Msi-1 (**C**), BrdU/GFAP (**F**), and BrdU/DCX (**I**). Most BrdU-positive cells expressed Msi-1, but only a few expressed GFAP (D–F). About half of BrdU-positive cells expressed DCX. BrdU-plus-DCX-positive cells are indicated with arrows, whereas BrdU-positive, DCX-negative cells are shown with arrowheads (G–I). Scale bar = 50 μm.

TABLE I. BrdU-Positive Cells and the Characteristic Phenotype 1 Day After BrdU Administration in Ischemic and Nonischemic Control Mice

	Total BrdU(+) cells/mm^2	BrdU(+) Msi-1(+)/total BrdU(+) (%)	BrdU(+) GFAP(+)/total BrdU(+) (%)	BrdU(+) DCX(+)/total BrdU(+) (%)
Control	21.6 ± 10.7	94.7 ± 4.1	10.5 ± 5.4	55.8 ± 14.6
Ischemia	106.0 ± 21.1	95.8 ± 2.3	16.1 ± 6.9	48.8 ± 14.0

All mice subjected to ischemia showed neuronal loss in the hilus of the dentate gyrus (Fig. 1G–I).

Characteristics of Proliferating Cells in the Mouse Hippocampus After Ischemia

To determine the phenotype of BrdU-positive cells in the SGZ 1 day after BrdU administration, double immunofluorescence for BrdU/Msi-1, BrdU/GFAP, or BrdU/DCX was evaluated (Fig. 2). In both nonischemic controls and ischemic mice, most BrdU-positive cells in the SGZ coexpressed Msi-1 (94.7 ± 4.1% in control mice and 95.8 ± 2.3% in ischemic mice; Fig. 2A–C, Table I), whereas only 10–15% of BrdU-positive cells exhibited GFAP (10.5 ± 5.4% in control mice and 16.1 ± 6.9% in ischemic mice; Fig. 2D–F, Table I). Roughly half of BrdU-positive cells in the SGZ showed colocalization with DCX (55.8 ± 14.6% in control mice and 48.8 ± 14.0% in ischemic mice; Fig. 2G–I, Table I).

We examined further progenitor cell differentiation at 14 or 30 days after BrdU administration by double immunofluorescence for BrdU/β-tubulin III, BrdU/NeuN, BrdU/MAP2, or BrdU/GFAP. Most BrdU-positive cells exhibited neuronal phenotypes (Figs. 3 and 4). By semiquantitative analysis, more than 80% of BrdU-positive cells in the SGZ and GCL exhibited NeuN in both groups (83.6 ± 5.7% in control mice and 89.9 ± 4.0% in ischemic mice; Table II). In contrast, only 5–15% of BrdU-positive cells in the SGZ and GCL were colabeled with GFAP (12.6 ± 3.1% in control mice and 5.8 ± 4.7% in ischemic mice; Fig. 3, Table II).

Next, we examined whether these nascent BrdU-positive neurons could be integrated into neural circuits. New BrdU-positive granular cells expressing the mature neuronal marker MAP2 extended the dendritic processes toward and into the molecular layer (Fig. 4A–F).

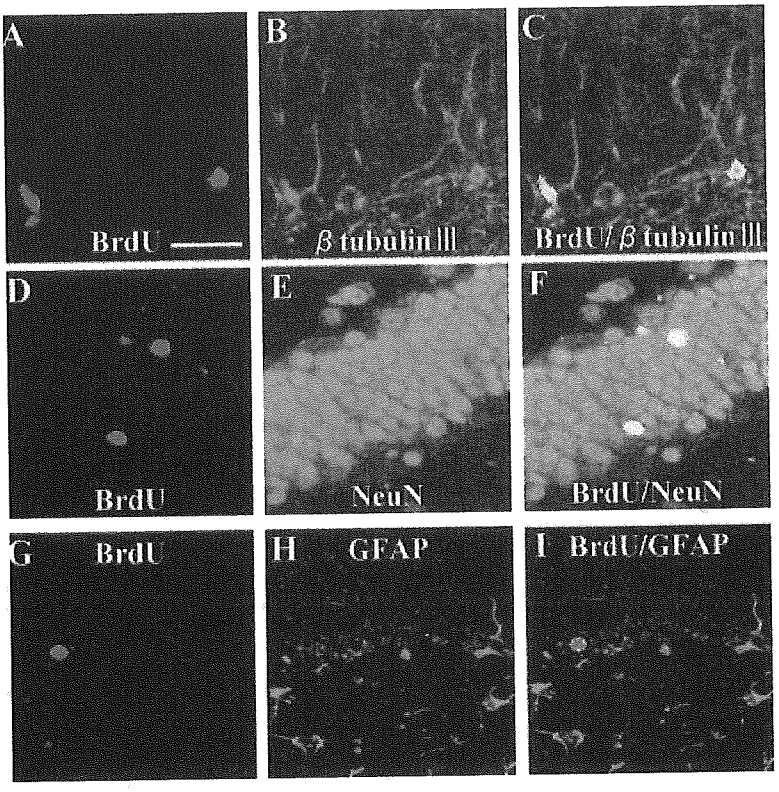

Fig. 3. Neuronal differentiation of newly formed cells in the SGZ and GCL after ischemia. BrdU (50 mg/kg, i.p.) was administered 9 days after ischemia, and mice were killed 14 (**A–C**) or 30 days (**D–I**) after BrdU administration. At 14 days after BrdU administration, most BrdU-positive cells expressed immunoreactive β-tubulin III (A–C). At 30 days after BrdU administration, most BrdU-positive cells expressed NeuN (D–F). In contrast, few BrdU-positive cells exhibited GFAP immunoreactivity in the SGZ and GCL (**G–I**). Scale bar = 40 μm.

TABLE II. Differentiation into Neuron and Astrocyte and Survival 30 Days after BrdU Administration in Ischemic and Nonischemic Control Mice

	Total BrdU(+) cells/mm^2	BrdU(+) NeuN(+)/total BrdU(+) (%)	BrdU(+) GFAP(+)/total BrdU(+) (%)
Control	4.7 ± 4.8	83.6 ± 5.7	12.6 ± 3.1
Ischemia	38.7 ± 13.1	89.9 ± 4.0	5.8 ± 4.7

COX-2 Expression in the Mouse Hippocampus

In control animals, COX-2 immunoreactive neurons were found in the CA4 sectors and the dentate gyrus (Fig. 5A–C). At 10 days after ischemia, the level of neuronal COX-2 immunoreactivity was almost the same as basal expression in dentate gyrus granular cells (Fig. 5D–I). Consistent with the previous finding that COX2 was localized in nuclear envelope and endoplasmic reticulum (Morita et al., 1995), COX-2 immunoreactivity in the neuron was observed in the perinuclear region in either control or 10 days after ischemia (Fig. 5A–I). Notably, COX-2 immunoreactivity was expressed in GFAP-positive hypertrophic reactive astrocytes in the hilus after ischemia (Fig. 5D–F), but not in control animals (Fig. 5A–C).

BrdU-positive cells in the SGZ did not express COX-2 in control or ischemic mice on the next day after BrdU administration (Fig. 6A –C). In addition, Msi-1-positive cells in the SGZ did not coexpress COX-2 (Fig. 6D–F). Thus, we concluded that the Msi-1- and BrdU-positive neuronal progenitors in the SGZ did not express COX-2.

COX Inhibitor Decreased the Proliferation of Progenitor Cells in SGZ after Ischemia

In nonischemic control mice, the number of BrdU-positive cells in vehicle, indomethacin, and NS-398 treated groups were 16.3 ± 10.5, 11.8 ± 5.7, and 13.7 ± 8.1/mm^2, respectively, (Fig. 7A, n = 6 mice in each group). In the ischemic group, mice treated with indomethacin and NS-398 showed a significant decrease in the number of BrdU-positive cells in the SGZ compared to vehicle-treated mice at 10 days after ischemia (56.0 ± 30.3/mm^2 in mice treated with vehicle, 35.6 ± 22.0/mm^2 in mice treated with indomethacin, and 34.2 ± 25.8/mm^2 in mice treated with NS-398; Fig. 7A, n = 6 mice in each group).

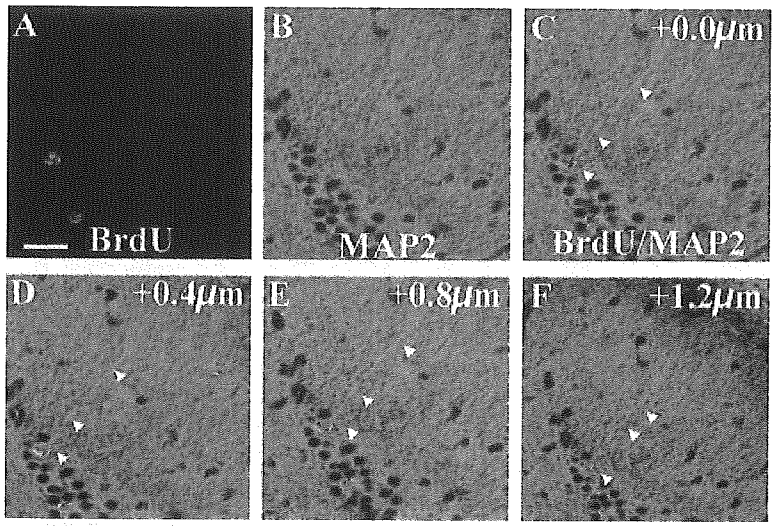

Fig. 4. New neurons extended dendritic processes. At 30 days after BrdU administration, BrdU-positive cells expressed MAP2 immunoreactivities (**A–C**). Z-series analysis (**D–F**) indicated that new cells colabeled with BrdU and MAP2 extended dendritic processes toward and into the molecular layer. Scale bar = 75 μm.

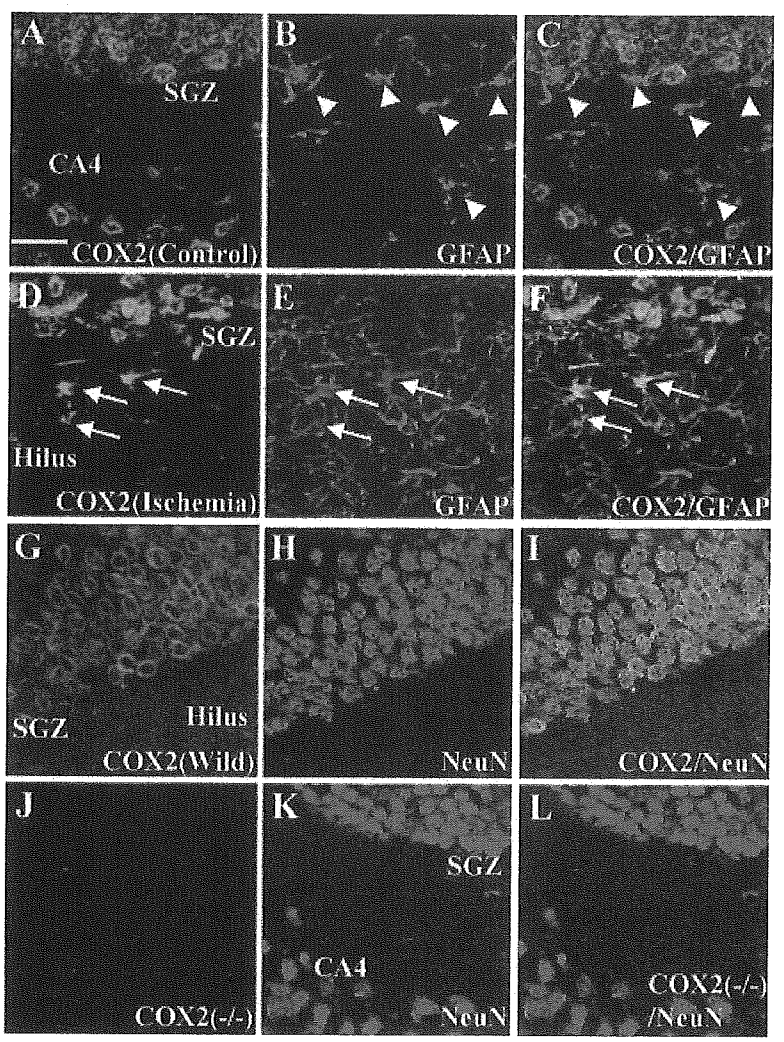

Fig. 5. COX-2 expression was demonstrated in neurons and reactive astrocytes, and not induced in COX-2 knockout mice. Presence or absence of COX-2 immunoreactivity is shown in neurons and astrocytes in the SGZ and hilus in control and 10 days after ischemia. BrdU was administered in controls and 9 days after ischemia. In control mice, COX-2 immunoreactivity was not expressed in astrocytes in the SGZ and hilus as indicated with arrowheads (**A–C**). On the other hand, in ischemic mice, COX-2 immunoreactivity was demonstrated in GFAP-positive hypertrophic reactive astrocytes as indicated with arrows (**D–F**) in addition to neurons (**G–I**). COX-2 immunoreactivity was not detected in COX-2 knockout mice (**J–L**). Merged images show (C,F) COX-2/GFAP and (I,L) COX-2/NeuN. Scale bar = 40 μm.

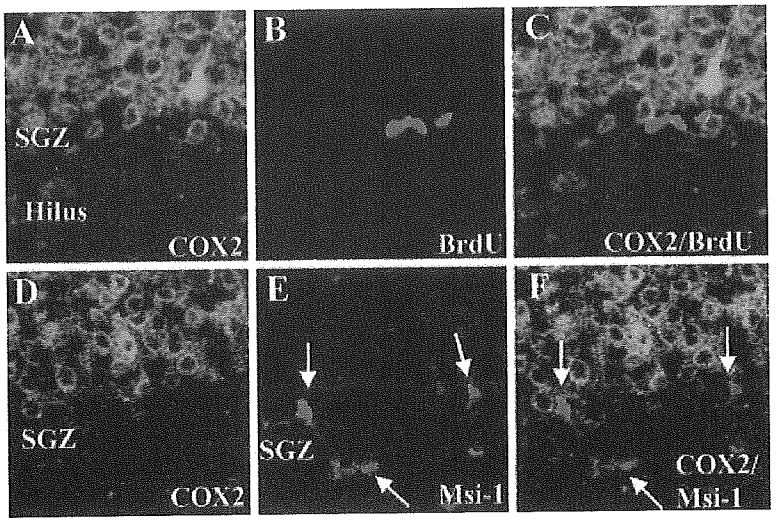

Fig. 6. COX-2 expression was not observed in neural progenitor cells. BrdU was administered 9 days after ischemia. Merged image (**C**) shows COX-2/BrdU; (**F**), COX-2/Msi-1. COX-2 immunoreactivity was not detected in BrdU-positive proliferating progenitor cells (**A–C**) nor in Msi-1-positive cells in the SGZ (**D–F**). Msi-1-positive, COX-2-negative cells are shown with arrows (D–F). Scale bar = 40 μm.

Progenitor Cells Proliferation in COX-2 Knockout Mice After Ischemia

In COX-2 knockout mice, COX-2 immunoreactivity was not observed in the control or in the ischemic hippocampus (Fig. 5J–L). In all COX-2 knockout mice subjected to ischemia, neuronal loss in the dentate hilus was observed similarly (Fig. 1I). In nonischemic control mice, numbers of BrdU-positive cells in the SGZ of COX-2 +/+, +/−, and −/− mice were 23.3 ± 8.7/mm^2, 17.7 ± 7.5/mm^2, and 14.5 ± 6.2/mm^2, respectively (Fig. 7B).

In the ischemic groups, BrdU-positive cells in the SGZ 10 days after ischemia in COX-2 +/+ mice were significantly more numerous (79.6 ± 32.5/mm^2) than in COX-2 +/+ nonischemic control mice (about 3.5 times). Numbers of BrdU-positive cells after ischemic insults were significantly less in COX-2 +/− (48.3 ± 24.6/mm^2) and COX-2 −/− mice (39.3 ± 21.2/mm^2) than in COX-2 +/+ mice (Fig. 7B).

DISCUSSION

Our data demonstrated that transient forebrain ischemia increased neurogenesis in the dentate gyrus of the adult mouse hippocampus. The postischemic enhanced proliferation of neural progenitor cells in the SGZ was attenuated by COX inhibitors and in COX-2 knockout mice.

Increased Neurogenesis by Progenitor Cells in the Ischemic Mouse Hippocampus

Consistent with previous reports using a global ischemia model (Liu et al., 1998; Takagi et al., 1999; Yagita et al., 2001), the number of BrdU-positive cells in the SGZ peaked 10 days after ischemia. On the day after BrdU injection, most BrdU-positive cells in the SGZ also expressed Msi-1, and about half of those cells exhibited DCX; however, only about 10% of BrdU-positive cells coexpressed GFAP. Msi-1 is highly enriched in neural progenitor/stem cells and astrocytes (Sakakibara et al., 1996; Sakakibara and Okano, 1997; Kaneko et al., 2000). In the present study, BrdU- and Msi-1-positive but GFAP-negative cells were identified as neural progenitor cells (Yagita et al., 2001; Takasawa et al., 2002). A recent report, however, suggested that GFAP-positive astrocytes in the SGZ generated new neurons via GFAP-negative intermediate neuronal progenitor cells in the adult mammalian hippocampus (Seri et al., 2001). Because conversion to the GFAP-negative intermediate progenitors was rapid (Seri et al., 2001), many of the BrdU-positive cells were already GFAP-negative 24 hr after BrdU administration in the present study. Because recent experiments using both neurosphere and a monolayer culture method suggested that the adult dentate gyrus did not contain resident neural stem cells (Seaberg and van der Kooy, 2002), the progenitor or stem cells in the SGZ, therefore, must be identified carefully. DCX is a neural microtubule-associated protein associated with neuronal migration that is expressed in both migrating neuroblasts and immature neurons (Francis et al., 1999; Gleeson et al., 1999; Gu et al., 2000; Jin et al., 2001). Our results suggested that DCX also was expressed by a subset of neural lineage cells derived from Msi-1-positive neural progenitor cells in the ischemic hippocampus.

Newborn Neurons After Ischemic Insult Extend Dendrites

Newly generated neurons in the dentate gyrus of the adult hippocampus have been reported to send appropriate axonal projections to the CA3 sector under physiologic conditions (Markakis and Gage, 1999), and also after seizures (Parent et al., 1997). The newly generated neurons were integrated functionally into the hippocampal circuitry according to retroviral labeling (van Praag et al., 2002); however, whether cells newly generated in the SGZ after ischemic insult became functional remained unknown. We showed that BrdU- and MAP2-positive